



OPEN

Novel adult cortical neuron processing and screening method illustrates sex- and age-dependent effects of pharmaceutical compounds

Arthur Sefiani¹, Ivan Rusyn² & Cédric G. Geoffroy¹✉

Neurodegenerative diseases and neurotraumatic injuries are typically age-associated disorders that can reduce neuron survival, neurite outgrowth, and synaptic plasticity leading to loss of cognitive capacity, executive function, and motor control. In pursuit of reducing the loss of said neurological functions, novel compounds are sought that promote neuron viability, neuritogenesis, and/or synaptic plasticity. Current high content in vitro screenings typically use cells that are iPSC-derived, embryonic, or originate from post-natal tissues; however, most patients suffering from neurodegenerative diseases and neurotrauma are of middle-age and older. The chasm in maturity between the neurons used in drug screens and those in a target population is a barrier for translational success of in vitro results. It has been historically challenging to culture adult neurons let alone conduct screenings; therefore, age-appropriate drug screenings have previously not been plausible. We have modified Miltenyi's protocol to increase neuronal yield, neuron purity, and neural viability at a reduced cost to expand our capacity to screen compounds directly in primary adult neurons. To our knowledge, we developed the first morphology-based screening system using adult cortical neurons and the first to incorporate age and sex as biological variables in a screen using adult cortical neurons. By using primary adult cortical neurons from mice that were 4 to 48 weeks old for screening pharmaceutical agents, we have demonstrated age- and sex-dependent effects on neuritogenesis and neuron survival in vitro. Utilizing age- and sex-appropriate in vitro models to find novel compounds increasing neuron survival and neurite outgrowth, made possible by our modified adult neuron processing method, will greatly increase the relevance of in vitro screening for finding neuroprotective compounds.

The median age is rising worldwide¹ as a larger percentage of the population reaches late adulthood. In the United States from 1900 to 1996, the number of people over 65 years old increased by 11-fold, and the number of people over 85 years old increased by 31-fold². The percent of the population over 65 doubled from 8% in 1950 to 16% in 2018³. Both the absolute and relative number of older individuals are rising, which increases the prevalence of age-associated neurological disorders such as neurodegenerative disorders and neurotrauma. From the year 1990 to 2010, dementia cases worldwide increased by 99.3% and the per capita rate for dementia worldwide increased by 53.3%⁴. The prevalence of traumatic brain injury (TBI) in senior citizens increased 53.5% from 2001 to 2010, as it simultaneously decreased for young adults⁵. From 1978 to 2005, the percentage of people with spinal cord injury (SCI) being of geriatric age increased by 267%⁶. Therefore, there is a growing need for developing novel therapeutic strategies specifically for protecting cognitive abilities in the older population.

In the search for novel medicines for neurodegenerative diseases and neurotrauma, researchers are looking for compounds that increase neuron survival and neurite regenerative capacity. The survival of neurons decreases after the onset of neurodegenerative diseases⁷ and neurotrauma^{8,9}, escalating the pathological and neurobehavioral outcomes. Because humans have an extremely limited capacity to regenerate neurons¹⁰, compounds that promote neuron viability are of great interest to mitigate neuron loss and associated disease conditions. In the

¹Department of Neuroscience and Experimental Therapeutics, School of Medicine, Texas A&M University, Bryan, TX 77807, USA. ²Department of Veterinary Integrative Biosciences, College of Veterinary Medicine & Biomedical Sciences, Texas A&M University, College Station, TX 77843, USA. ✉email: geoffroy@tamu.edu

case of SCI, there are several neuroprotective agents undergoing clinical trials, such as Riluzole¹¹, Glyburide¹², and Minocycline¹³. Although these compounds have unique mechanisms of action, their use is intended to prevent necrosis at the injury site and mitigate further neural degeneration¹⁴. For Alzheimer's disease, neuroprotective agents have been proposed to mitigate the deleterious effects of amyloid beta accumulation¹⁵.

Neurite growth is a vital step in the recovery process from neurotrauma to reconnect damaged connections¹⁶. In the case of SCI, axons extended from cortical neurons are damaged and degenerated, which then must be regenerated past the lesion site to restore connection to caudal neurons¹⁷. Neurodegenerative diseases also induce axonal degeneration which can lead to neuronal death and progression of pathology¹⁸. Current therapeutic strategies in neurodegenerative diseases, such as glaucoma and Parkinson's disease, aim at increasing axon regenerative capacity to mitigate pathology^{19,20}. Aging itself reduces neurite regenerative capacity²¹ and increases susceptibility of neurons to death and degeneration²², which can produce worse outcomes after neurotrauma²³ and increase the prevalence of neurodegenerative diseases^{24,25}. Therefore, it is imperative that novel therapeutic strategies can increase the survival and neurite regenerative capacity of neurons in older individuals as well.

An efficient way to identify compounds that increase the survival and neurite regenerative capacity of neurons is to perform high content in vitro screenings. To date, such screens have involved the use of cell lines, embryonic neurons, newborn neurons, and induced pluripotent stem cells (iPSC)-derived neurons^{26–30}. However, these neurons do not represent the target neuron population in humans in terms of age characteristics. Indeed, aged neurons have different characteristics relative to neurons from younger individuals^{21,22,31}. This dichotomy in age between in vitro assays and in vivo settings is likely to play a role in the high number of failures when moving a drug forward along the clinical phases. There is an age-dependent decline in axon growth after neurotrauma³² demonstrating the importance of age-appropriate models in pre-clinical studies. In fact, the age factor and associated complications have been advanced as a major component of the translational failure of promising drugs in the stroke field^{33,34} where most of the pre-clinical testing are performed in very young stroke models while human patients are older^{35,36}. Additionally, the same drug may have completely opposite effects depending on age, as is the case for methylphenidate which is used to treat attention deficit-hyperactivity disorder³⁷. Therefore, the age factor must be considered a vital biological variable starting from the in vitro screening process.

There are also sex-based differences in pharmacological response³⁸, pharmacodynamics, and pharmacokinetics³⁹; women are 50–75% more likely to experience an adverse reaction to prescription medication⁴⁰. Because of the disparity of prevalence between sexes for certain diseases, such as the disproportionality higher SCI incidence rate in men⁴¹ and prevalence of stroke in young women⁴², it is vital to understand sex based efficacy of compounds before moving onto clinical stages. Screening in embryonic or early postnatal neurons cannot properly take sex into account as sex differences in motor performance⁴³ and brain characteristics⁴⁴ are more apparent after puberty. Therefore, screening compounds on adult neurons in vitro at different age and in both sexes should be the first step in identifying the potential of compounds to enhance neuron survival and neurite growth, increasing the potential of translation success while minimizing possible harm.

Another potential hurdle in translating in vitro screening data to the development of therapeutics for human patients is the species of the cellular model used. Human neurons do differ significantly from that of rodents⁴⁵. Therefore, it would be ideal to conduct drug screenings in human neural cells. Currently, there are studies using the patient's own cells to create iPSCs with the patient's own unique genetic code^{46,47}. While promising and offering several advantages, the use of iPSCs-derived neurons for phenotypic screen purposes presents various challenges, including obtaining enough iPSCs-derived neurons for HCS, the cost of the screen, and more importantly, the inclusion of the age factor, which is one of the most vital components in the loss of regenerative capacity⁴⁸. Indeed, iPSC-derived neurons mimic the neurons of a developing embryonic brain with an immature electrophysiological profile⁴⁹. Use of human adult neurons would alleviate this issue, but is not compatible with HCS⁵⁰. Another possibility to tackle the interspecies problem would be to perform HCS in adult cortical neurons from large animals (e.g., sheep, pigs, monkeys) to provide confirmation of the results obtained screening in rodents. This would not guarantee the findings will be clinically translatable but could significantly increase the odds as the targets of interest are more likely to be of highly conserved regions shared with humans. Such technology remains to be developed. Because adult neurons from rodents lose regenerative capacity with age^{21,32,50,51}, they may represent, to date, until screenings in larger adult animals are developed, the best option for HCS aiming at finding drugs promoting neuron survival and neuroregeneration.

To date, culturing even young adult cortical neurons has been challenging. The few protocols existing lead to very inconsistent results, with a low yields and cell viability^{52–54}. This makes it very difficult, if not impossible, to test a single drug candidate on young adult neurons, let alone to test it on older cortical neurons (> 6 months). Using adult cortical neurons for an age- and sex-appropriate compounds screen in vitro has therefore not been conceivable yet, but it would be immensely beneficial to find demographic-appropriate drug candidates. Miltenyi recently developed a system to culture very young adult brain neurons (up to 4 weeks old)^{53,55–57}. We modified this technique to culture middle- and advanced-age cortical neurons²¹. In the present report, we further adapted this protocol to screen for compounds that enhance survival and neurite outgrowth and determine the demographic the compounds have most efficacy in. Indeed, positive hits from embryonic or postnatal cortical neurons may not affect older neurons, and it is plausible that compounds with no effect on embryonic or postnatal neurons may in fact present beneficial effects on adult neurons only. Therefore, screens utilizing adult cortical neurons may present compounds that have been prematurely dismissed as false negatives in previous screens. Developing such a system would also allow for the examination of sex-dependent effects of compounds, an essential variable in drug development⁵⁸. This may allow for the development of future age- and sex-based personalized medicine.

Our newly developed protocol increases the number of viable neurons obtained per gram of brain tissue and significantly increases the absolute volume of brain tissue an individual can process solitarily. We designed a screening and analysis workflow to minimize human input to mitigate human biases. Through a targeted screen (testing of pre-selected drugs known to promote neuron survival/regeneration) using our novel model,

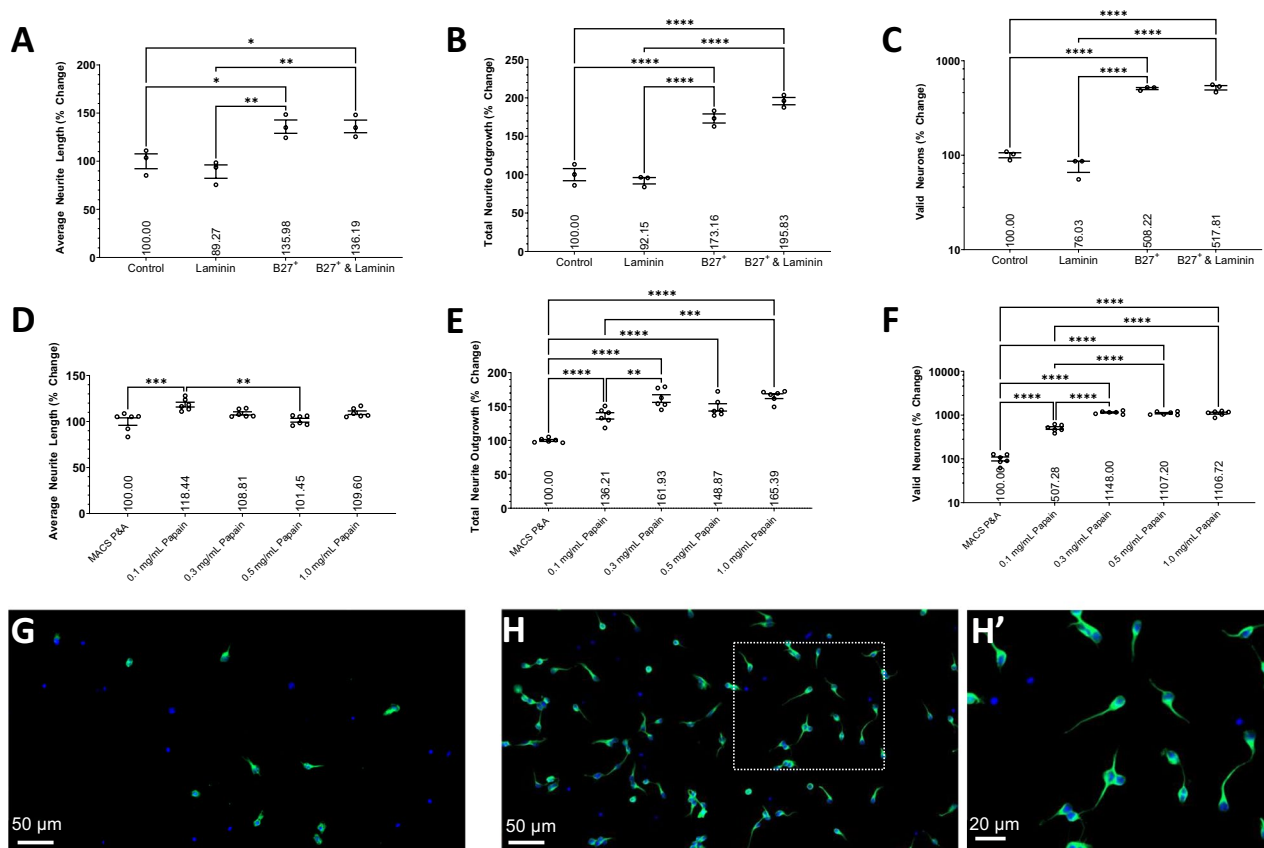


Figure 1. The effects of Laminin coating and media supplementation and different digestion enzymes. Histograms of the (A) average neurite length, (B) total neurite outgrowth, and (C) number of valid neurons expressed as percent change relative to the control group containing no B27⁺ supplement or laminin coating. Primary cortical neurons isolated from young adult male mice and cultured for 2DIV. 3 wells per condition. Histograms of the (D) average neurite length, (E) total neurite outgrowth, and (F) number of valid neurons expressed as percent change relative to the MACS P&A group. Data analyzed using one-way ANOVA with Tukey's post-hoc test comparing the mean of each condition to one another. Representative $\times 20$ magnification images of primary cortical neurons isolated using the (G) MACS P&A and (H) 0.3 mg/mL Papain (H') $\times 63$ magnification) dissociation enzymes from young adult male mice and cultured for 2DIV; stained with TUBB3 (Green) and DAPI (Blue). 6 wells per condition (n=6). * (P < 0.05), ** (P < 0.01), *** (P < 0.001), **** (P < 0.0001). Graphs show mean and SEM. Scale Bar = 50 μ m (D,E) or 20 μ m (E').

we identified compounds with age- and sex-dependent effects on neuron survival and neurite outgrowth. This clearly illustrates the need to perform future screens in different age and sex groups (1) to determine the specific demographic the compound will have most clinical effect in; (2) to theoretically prevent the premature dismissal of compounds with no effect in iPSC/embryonic screens yet would be advantageous to adults; and (3) to reduce the false positivity rate from iPSC/embryonic screens by efficiently vetting compounds that do not show benefit to adult neurons and therefore will likely not be efficient when testing in preclinical settings.

Results

The original protocol from Miltenyi has been extensively modified and optimized to fit various drug screening criteria, by processing larger amount of tissue, expediting the process, reducing costs, and providing researchers with a new tool that can potentially provide more clinically relevant data than previous conventional screening methods. Importantly, we demonstrated the utility of this system by illustrating the sex and age-dependent effects of 2 compounds.

Optimization of surface coating and media supplementation. We first determined if laminin coating in addition to the PDL would improve neurite outgrowth and number of valid neurons and/or mitigate the need for extra supplementation of media with B27⁺. Primary cortical neurons isolated from young adult male mice, using the original Miltenyi protocol⁵⁹, were cultured at 10,000 cells/well for 2DIV on PDL or PDL/laminin coated wells with or without B27⁺. The B27⁺ supplementation significantly increased the average neurite length (Fig. 1A, P < 0.05), total neurite outgrowth (total neurite outgrowth, P < 0.0001), and number of valid neurons (Fig. 1C, P < 0.0001). The presence of laminin did not improve neurite growth or the number of valid neurons, nor can it replace or enhance media supplementation. Plating neurons without PDL coating resulted in few

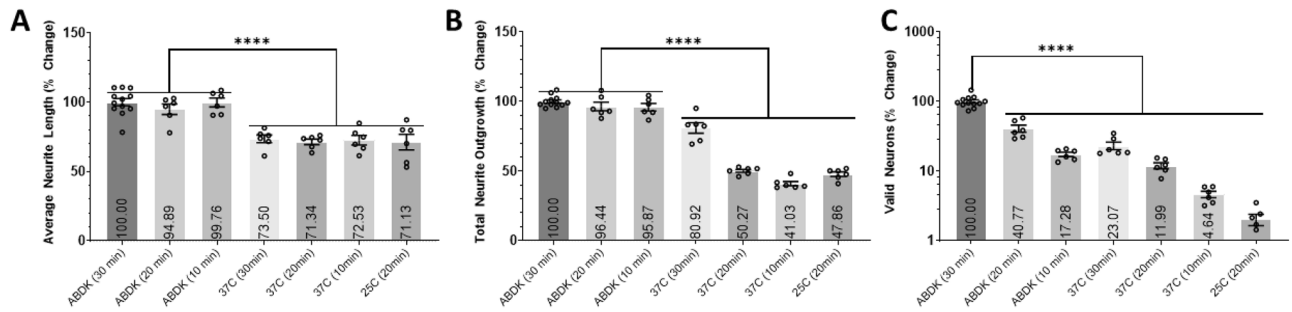


Figure 2. The effects of different dissociation protocols, timing, and temperature. Histograms of the (A) average neurite length, (B) total neurite outgrowth, and (C) number of valid neurons expressed as percent change relative to the standard gentleMACS Program 37C_ABDK_01 protocol (ABDK (30 min)). Data analyzed using one-way ANOVA with Dunnett's post-hoc test comparing the mean of each condition to the mean of ABDK (30 min). In parentheses represents the length of the protocol whether being ran on the gentleMACS™ Octo Dissociator with Heaters (ABDK) or in a revolving apparatus incubated at 37 °C or 25 °C. Primary cortical neurons isolated from young adult male mice and cultured for 2DIV. 6 wells per condition (n = 6). *(P < 0.05), ***(P < 0.001), ****(P < 0.0001). Graphs show mean and SEM.

neurons adhering to the surface without substantial neurite growth (data not included). Media supplementation and surface coating is required, especially to increase the number of valid adult cortical neurons. Only PDL coating was used for subsequent experiments and all experimentation was done in standard size 384-well plates.

Determine the best digestion enzyme. Next, we determined the effectiveness of different digestion enzymes and concentrations to use to isolate cortical neurons and their efficacy to maintain their viability. Identical dissection method, dissociation method and temperature, and volumes of digestive enzymes were used herein. After the respective digestive enzymes were used in replacement of 0.3 mg/mL papain (“Methods” section) to isolate cortical neurons from young adult male mice (1 mouse cortex per condition), the neurons were evenly distributed between 6 wells and cultured for 2DIV to measure how many cortical neurons can be extracted using each digestive enzyme and their ability to maintain neuron viability (Fig. 1D–H). Overall, papain presented beneficial effects on cell survival and neurites outgrowth compared to the MACS⁺ P&A digestive enzyme. 0.3–1.0 mg/mL papain resulted in increased total neurite outgrowth (P < 0.0001) and number of valid neurons (P < 0.0001) when compared to MACS⁺ P&A. 0.1 mg/mL papain had significantly higher total neurite outgrowth and number of valid neurons compared to MACS⁺ P&A (P < 0.0001), yet significantly lower values relative to higher papain concentrations (P < 0.0001). This suggests digesting with papain has a dose-dependent effect that plateaus at ≤ 0.3 mg/mL. Notably, 0.1 mg/mL papain had higher average neurite length compared to 0.5 mg/mL papain (P < 0.01) and MACS⁺ P&A (P < 0.001), although still had similar total neurite outgrowth compared to 0.5 mg/mL papain. There were no significant differences between papain concentrations of 0.3–1.0 mg/mL for any analysis, and therefore, the concentration of 0.3 mg/mL, the lowest effective papain concentration, was used for the remainder of the experiments to reduce cost and potential off-target effects induced by higher concentrations. Accutase⁺ and 0.25% Trypsin were also tested and yielded poorer outcomes compared to MACS⁺ P&A (data not included).

Determine the best dissociation method, timing, and temperature. Here, we determined the effectiveness of different digestion methods, the incubation timing of those methods, and the incubation temperatures on the dissociation of cortical tissue from young adult male mice. After the cortical neurons preparation with each respective protocol, the cells are evenly dispersed between 6 wells to analyze both the yield and viability of the neurons. We compared the standard protocol ABDK-30 min to ABDK-20 or 10 min (all in the Octo Dissociator with heaters at 37 °C) and to a revolving apparatus at different times and temperatures (Fig. 2). Neurons dissociated using the Octo Dissociator had longer average neurite lengths and total neurite outgrowth in comparison to neurons incubated in a revolving apparatus. The incubation time had no effect on neuron morphology when using Octo Dissociator, yet, when using a rotating apparatus, a reduction in time lead to reduced total neurite growth (P < 0.0001). The number of valid neurons was affected by method, timing, and temperature. Using the Octo Dissociator increased the number of valid neurons by approximately fourfold regardless of the incubation time relative to using a revolving apparatus at 37 °C (P < 0.0001). In each dissociation method, there was approximately a twofold increase in the number of valid neurons for every 10 min increase in incubation time (P < 0.0001). Furthermore, reducing the temperature from 37 to 25 °C during the 20 min incubation in a revolving apparatus reduced the number of valid neurons without impacting neuron morphology (P < 0.0001, Fig. 2C). The gentleMACS Program 37C_ABDK_01 protocol was used in the following experiments.

The effects of cell plating density. The reaction of neurons to compounds may be dependent on their plating density. Therefore, we assessed the effects of cell plating density of cortical neurons (from young adult male mice) on the average neurite length, total neurite outgrowth, and number of valid neurons per well (Fig. 3). (S)-H-1152 is a selective and potent rho-associated kinase (ROCK) inhibitor that attenuates KCl-induced con-

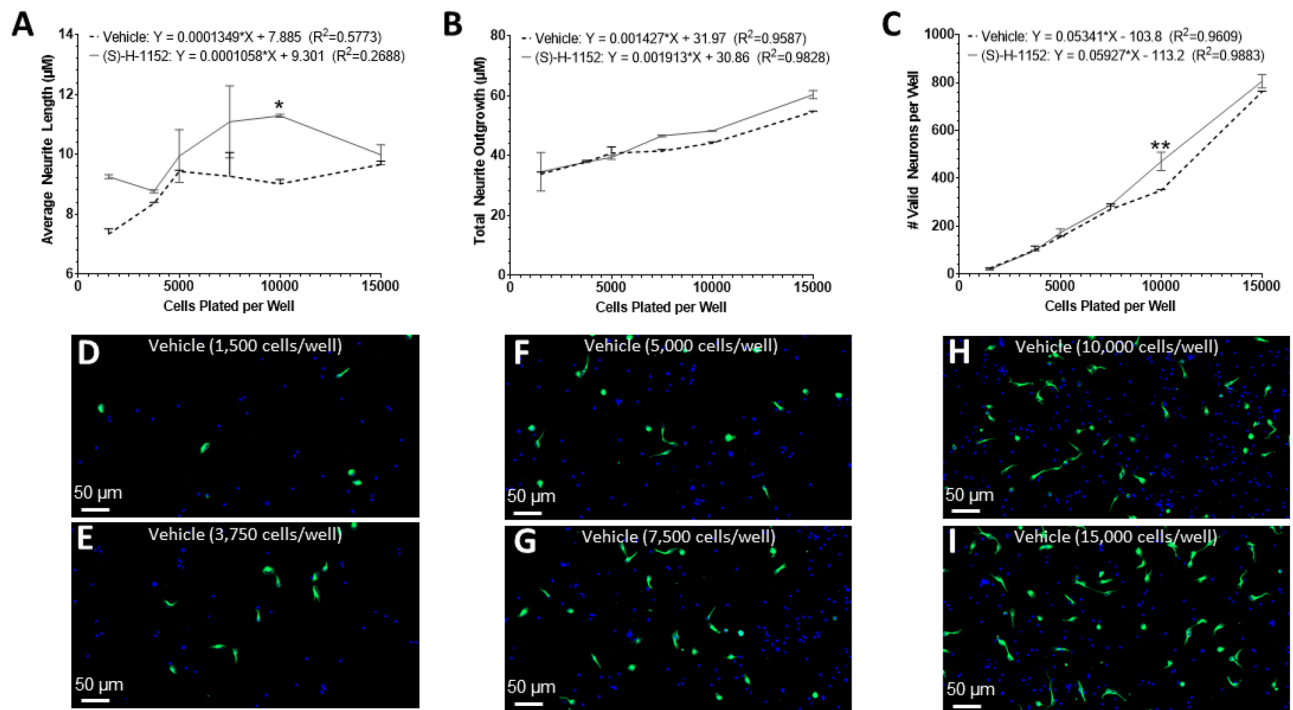


Figure 3. The effects of cell plating density. Linear trends of the (A) average neurite length, (B) total neurite outgrowth, and (C) number of valid neurons of Vehicle and (S)-H-1152 treated primary cortical neurons isolated from young adult male mice cultured for 2DIV. The X-axis denotes the number of cells plated in each well. Representative $\times 20$ magnification images of primary cortical neurons from young adult male mice treated with Vehicle for 2DIV and plated at (D) 1500 cells/well, (E) 3750 cells/well, (F) 5000 cells/well, (G) 7500 cells/well, (H) 10,000 cells/well, and (I) 15,000 cells/well; stained with TUBB3 (Green) and DAPI (Blue). Two-way ANOVA with Sidák's multiple comparisons test was used to compare the means of neurons with different treatments for each respective plating density denoted by * ($P < 0.05$), ** ($P < 0.01$), *** ($P < 0.001$), **** ($P < 0.0001$). Simple linear regression conducted to determine goodness of fit and if the slope differs significantly from 0. Linear regression t-test was used to compare the slope of the regression lines. 2 wells per condition ($n = 2$). Graphs show mean and SEM. Scale Bar = 50 μm .

tractions of femoral arteries⁶⁰ and augments neurite outgrowth in dorsal root ganglion cells isolated from 1-day old rats that are cocultured with Schwann cells^{61,62}. No significant correlation was found in the linear regression between plating density and the average neurite outgrowth for both 0.05% DMSO (dimethyl sulfoxide, Vehicle) and 5 μM (S)-H-1152 treated groups. There was a significant positive correlation between both total neurite outgrowth (P values: Vehicle < 0.001 , (S)-H-1152 < 0.0001) and number of valid neurons per well (P values: Vehicle < 0.001 , (S)-H-1152 < 0.0001) and the cell plating density for both treatment groups. Only the slope of the total neurite outgrowth linear regression line differed significantly between treatment groups, (S)-H-1152 induced a steeper increase in total neurite outgrowth and therefore more responsive to increased plating density ($P < 0.05$). (S)-H-1152 significantly increased the average neurite length ($P < 0.05$) and number of valid neurons ($P < 0.01$) compared to DMSO control only when 10,000 cells were plated per well. Therefore, plating density can determine which compounds are deemed positive hits and must be taken into consideration during screenings. The number of valid neurons for both Vehicle ($R^2 = 0.9911$) and (S)-H-1152 ($R^2 = 0.9923$) increases exponentially. Therefore, there may be extrinsic factors related to plating density that augment the neurite formation and/or survival of neurons. To minimize the impact of these factors when screening for new compounds, which may hinder the effect of the tested drugs, the concentration of 10,000 neurons per well appears the best choice and was used in the rest of the experiments.

The efficacy of various neuronal supplements. To improve the survival of neurons and create an environment that resembles in vivo conditions, neuron supplements are added to media to study the synaptic function, neurite growth, and survival of primary neurons in vitro in a chemically defined manner without the use of serum^{63–66}. Here, we determined the efficacy of NeuroBrew²¹, B27⁺, and NeuroCultSM SM1 as serum-free neuronal supplements to support neuron survival and neurite outgrowth of cortical neurons from young adult male mice (Fig. 4). The use of B27⁺ resulted in an increase in the average neurite length ($P < 0.0001$), total neurite outgrowth ($P < 0.001$), and number of valid neurons ($P < 0.05$) relative to all other cohorts. Therefore, B27⁺ will be used in future screenings to better nurture the adult neurons. The potential issue in using B27⁺ is the fact that it may mask the true effects of compounds due to its increased potency to augment survival and neurite growth compared to other supplements, although, compound screenings cannot be done in neurons that are not viable and reactive to drug treatment. On another note, there may be ingredients in the supplement that counteract

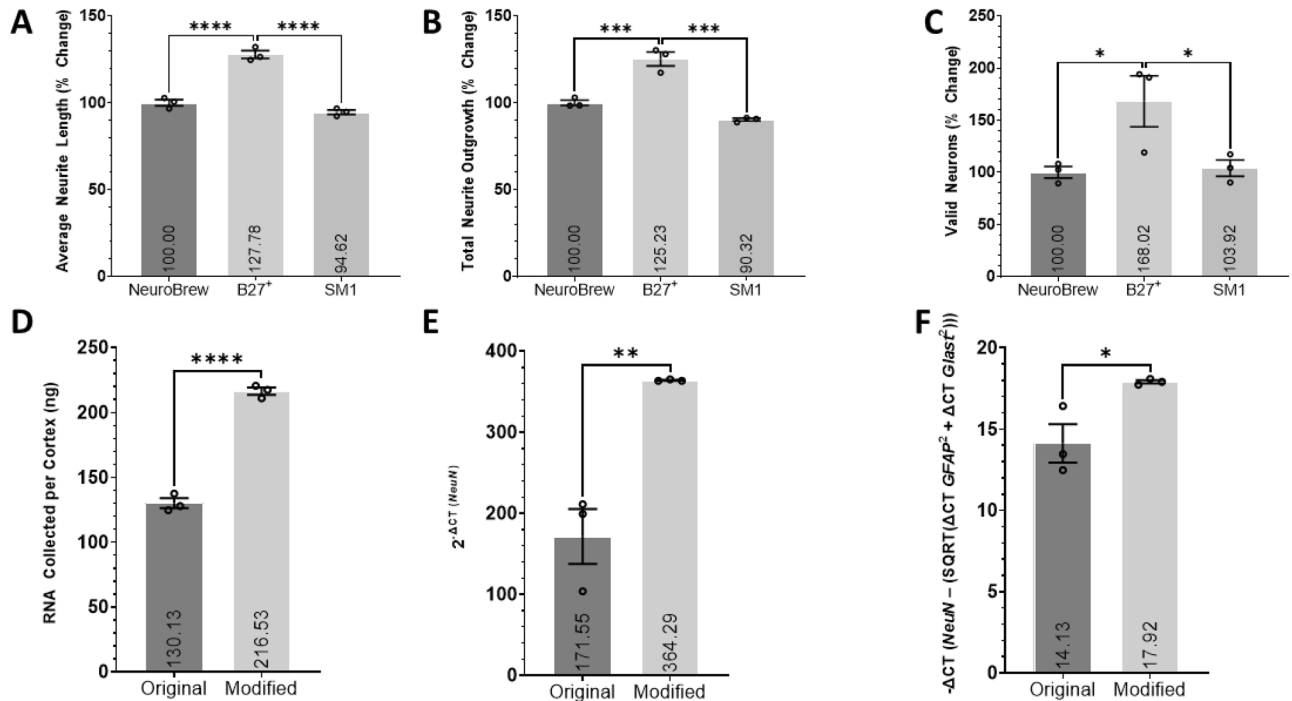


Figure 4. The efficacy of various neuronal supplements and culture purity assessed with RNA expression analysis. Histograms of the (A) average neurite length, (B) total neurite outgrowth, and (C) number of valid neurons of primary cortical neurons treated with the respective neuronal supplement isolated from young adult male mice and cultured for 2DIV. Data is expressed as percent change relative to the B27⁺ supplement cohort. Data analyzed using one-way ANOVA with Dunnett's post-hoc test comparing the mean of each condition to the mean of the B27⁺ supplement group. 3 wells per condition. Histograms of the (D) mass of RNA collected from each preparation, (E) the relative expression of *NeuN* expressed as 2^{-ΔCT} (*NeuN*) and (F) the relative expression of *NeuN* in relation to *GFAP* and *Glast* comparing the original protocol from Miltenyi (Original) and our finalized modified protocol (Modified). $-\Delta CT = -(\Delta CT \text{ NeuN} - (\text{SQRT}(\Delta CT \text{ GFAP}^2 + \Delta CT \text{ Glast}^2)))$. All ΔCT values are calculated as follows: $\Delta CT \text{ Primer} = CT \text{ Primer (Sample)} - CT \text{ Primer (Negative Control)}$. Student's T-test was used to compare the means of each cohort. RNA extracted from primary cortical neurons isolated from young adult male mice following the original and modified protocol. 3 independent samples per cohort, each analyzed in triplicate (n = 3). * (P < 0.05), ** (P < 0.01), *** (P < 0.001), **** (P < 0.0001). Graphs show mean and SEM.

potentially beneficial compounds or conceal their effects, therefore, we aim to minimize the need for supplementation and only use the recommended concentration of 1×.

Culture purity assessed with RNA expression analysis. The differences between the original and modified neuron isolation, processing, and culturing protocols are evident in the analysis for neurite outgrowth and valid neurons. These modifications have allowed for the culturing and screening of older adult cortical neurons. We performed RNA expression analysis on cortical neurons extracted from young adult male mice using RT-qPCR to determine how these modifications have affected the culture purity, by assessing RNA yield, neuron specific yield, and purity (Fig. 4). The RT-qPCR data indicates that the modified protocol resulted in significantly more RNA being isolated from each cortex (P < 0.0001), greater *NeuN* expression from the isolated cells (P < 0.01), and increased *NeuN* expression relative to *GFAP* and *GLAST* (P < 0.05). The in vitro cultures were suggestive of the modified protocol containing more cells; this data confirms that not only are more cells isolated, but a larger percentage of those cells are neurons. The modified protocol increased RNA yield by only 66% (Fig. 4A) yet increased the *NeuN* expression by 112% (Fig. 4B), suggesting an unproportionally larger increase in neurons relative to other neural cells. This was confirmed by the significant increase in the relative *NeuN* expression in the modified protocol compared to the combination of *GLAST* and *GFAP* expression (Fig. 4C). To confirm with immunocytochemistry, we stained the cell cultures at 2DIV with GFAP and Iba1 and found none of the cells to be positive for either marker in either method (data not shown).

The effects of the vehicle DMSO. Due to the ability of DMSO to dissolve hydrophobic compounds⁶⁷, it is commonly used as a vehicle in high content screenings^{68,69}. To determine the tolerance of adult neurons to DMSO, we plated primary cortical neurons from young adult male mice in presence of different concentrations of DMSO using the modified protocol (Fig. 5). As expected, there was significant negative correlation

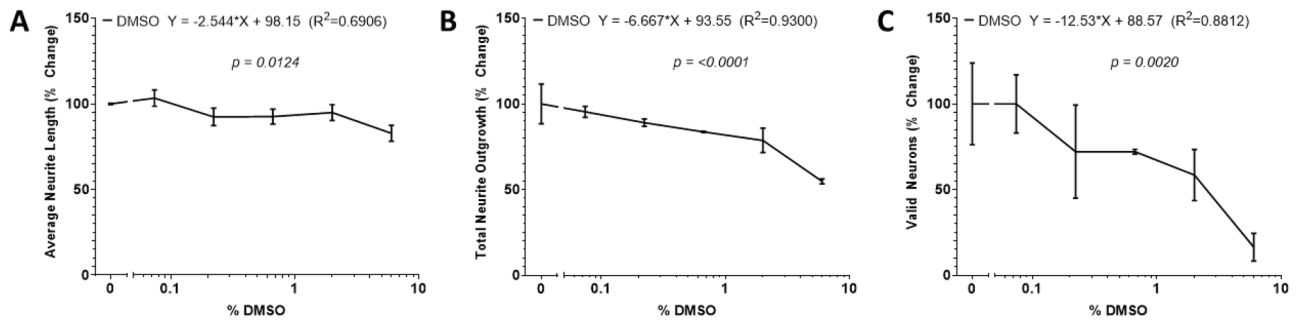


Figure 5. The effects of the drug vehicle DMSO. Linear trends of the (A) average neurite length, (B) total neurite outgrowth, and (C) number of valid neurons of primary cortical neurons isolated from young adult male mice cultured in various percentages of DMSO for 2DIV. The X-axis denotes the percentage of the neuron media comprising of DMSO. The values are expressed as percent change relative to the 0% DMSO cohort. Simple liner regression conducted to determine P value, goodness of fit, and if the slope differs significantly from 0.2 wells per condition (n = 2). Graphs show mean and SEM.

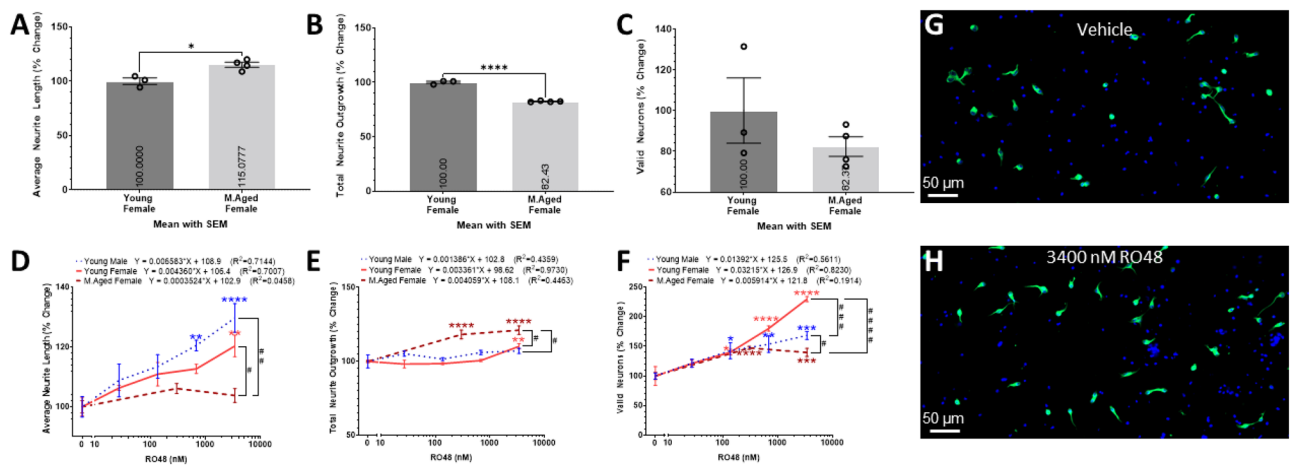


Figure 6. Sex and age-dependent effects of RO48. Histograms of the (A) average neurite length, (B) total neurite outgrowth, and (C) number of valid neurons extracted from the Vehicle treated group from figures (A–C), respectively, expressed as percent change relative to the young adult female (Young Female) cohort. Data analyzed using student’s T-test comparing the means of each cohort denoted by * ($P < 0.05$), ** ($P < 0.01$), *** ($P < 0.001$), **** ($P < 0.0001$). Linear trends of the (D) average neurite length, (E) total neurite outgrowth, and (F) number of valid neurons of primary cortical neurons isolated from young adult male, young adult female, and middle-aged female mice cultured in various concentrations of RO48 for 2DIV. The X-axis denotes the concentration (nM) of RO48 in the media (D–F). The values are expressed as percent change relative to the Vehicle treatment group of each cohort. Representative $\times 20$ magnification images of (G) Vehicle and (H) 3400 nM RO48 treated primary cortical neurons isolated from middle-aged female mice and cultured for 2DIV; stained with TUBB3 (Green) and DAPI (Blue). Simple liner regression was conducted to determine goodness of fit and if the slope differs significantly from 0. Linear regression t-test was used to compare the slope of the regression lines. Two-way ANOVA with Šidák’s multiple comparisons test was used to compare the means of neurons treated with 3400 nM RO48 between cohorts denoted by # ($P < 0.05$), ## ($P < 0.01$), ### ($P < 0.001$), #### ($P < 0.0001$) and to compare the means of neurons treated with various concentrations of RO48 to the Vehicle treatment group of the respective cohort denoted by * ($P < 0.05$), ** ($P < 0.01$), *** ($P < 0.001$), **** ($P < 0.0001$). All cohorts have equal parts Vehicle in media (0.05% DMSO). 3 wells per condition (n = 3). Graphs show mean and SEM. Scale Bar = 50 μ m.

between average neurite length ($P < 0.05$), total neurite outgrowth ($P < 0.01$), and number of valid neurons per well ($P < 0.01$) and the percentage of the media containing DMSO (% DMSO).

Sex and age-dependent effects of RO48 and culturing methods. We analyzed the effects of our isolation method, media, culturing protocol, and Vehicle against the young adult and middle-aged female cohorts. The middle-aged female cohort had a small but significant increase in average neurite length and significant decrease in total neurite outgrowth compared to the younger female cohort (Fig. 6A,B). The middle-aged female cohort has a non-significant downward trend in number of valid neurons compared to the younger

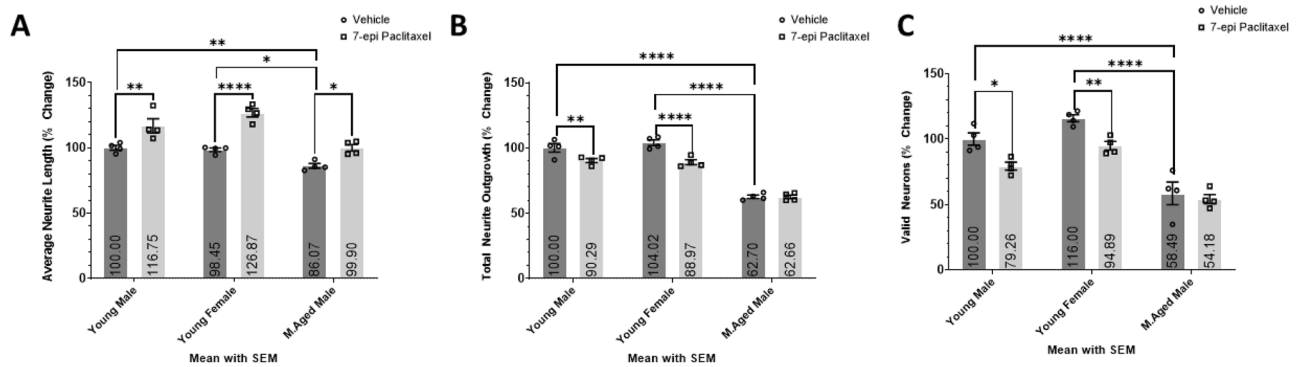


Figure 7. The age-dependent effects of 7-epi Paclitaxel. Histograms of the (A) average neurite length, (B) total neurite outgrowth, and (C) number of valid neurons expressed as percent change relative to the young adult male cohort with Vehicle treatment. Primary cortical neurons isolated from young adult male, young adult female, and middle-aged male mice cultured in Vehicle or 150 nM 7-epi Paclitaxel or 3DIV. Two-way ANOVA with Dunnett's multiple comparisons test was used to compare the means of each compound to the mean of the Vehicle treated group within each respective cohort. Two-way ANOVA with Tukey's multiple comparisons test was used to compare the mean of the Vehicle treated groups between different age cohorts. All cohorts have equal parts Vehicle in media (0.05% DMSO). 4 wells per condition ($n=4$). *($P<0.05$), **($P<0.01$), ***($P<0.001$), ****($P<0.0001$). Graphs show mean and SEM.

female cohort (Fig. 6C). RO48 activates mammalian target of rapamycin complex (mTORC)1/2 and phosphatidylinositol-3-kinase (PI3K) and decreases the phosphorylation of S6-926⁷⁰. RO48 has been shown to promote axon regeneration in vitro and augment axon growth and functional locomotor recovery in a rodent spinal cord injury model⁷¹. Therefore, RO48 is expected to provide neuroprotective qualities and/or augment neurite growth in our screen. There was a significant positive correlation between the RO48 concentration in the media and the total neurite outgrowth ($P<0.01$) and number of valid neurons ($P<0.05$) in the young adult female cohort only (Fig. 6D–H). The average neurite length (Fig. 6D) increased more, relative to the Vehicle, for the younger male and female cohorts compared to the middle-aged female cohort. The middle-aged female cohort was the only cohort without a significant increase in average neurite length at any concentration, resulting in a significant difference in the relative increase of neurite length at 3400 nM RO48 between the younger cohorts. For the total neurite outgrowth (Fig. 6E), the middle-aged female cohort has a significant increase in the neurite outgrowth compared to Vehicle treatment and significantly larger relative change compared to the younger cohorts. The young adult male and female cohorts do not differ significantly, although, the young adult female cohort does have a significant increase in neurite length at the highest dose. All 3 cohorts significantly increased the number of valid neurons at doses ≥ 300 nM, although, the relative increase from the Vehicle treatment differs significantly between all 3 cohorts (Fig. 6F). The young adult female cohort is most responsive, followed by the young adult male and middle-aged female cohort. This data elucidates the sex and age-dependent effects of RO48 on adult neurons in vitro which are more profound at higher RO48 concentrations. More importantly, it demonstrates the need to test compounds in both sexes and age groups to determine demographic specific efficacies.

The age-dependent toxicity of 7-epi Paclitaxel. 7-epi Paclitaxel is an FDA-approved drug for use in patients with ovarian cancer⁷². 7-epi Paclitaxel stabilizes microtubule bundles, impairs organelle transport⁷³, induces peripheral neuropathy through the CXCR1/2 pathway⁷⁴, and reduces brain injury after repeated traumatic brain injuries in mice by inducing neurite growth and nerve regeneration⁷⁵. Adult neurons isolated from the cortex of young adult male, young adult female, and middle-aged male mice were treated with 150 nM 7-epi Paclitaxel and Vehicle for 3DIV to analyze the average neurite length, total neurite outgrowth, and number of valid neurons (Fig. 7). 7-epi Paclitaxel significantly increases the average neurite length of all 3 age cohorts, yet only significantly decreases the total neurite outgrowth and number of valid neurons of the young adult cohorts without affecting the middle-aged male cohort. Therefore, screening 7-epi Paclitaxel in young adult neurons at 3DIV would yield an overall negative result while yielding an overall positive result in middle-aged male neurons suggesting a change in both the magnitude and direction of the effect. Studying the influence of 7-epi Paclitaxel in different demographics uncovers the need to conduct age-appropriate screenings to provide demographic-specific results and mitigate premature dismissal of potentially beneficial compounds.

Discussion

We developed a new screening platform utilizing primary adult mouse cortical neurons and demonstrated sex- and age-dependent effects of neuroactive compounds. This discrepancy between demographics supports the notion that future screenings must include both sexes and different age groups to account for sex- and age-dependent processes that may alter drug efficacy and even elicit opposite effects. Therefore, screening in multiple demographics is a necessary step in reducing unforeseen erroneous results and increasing confidence in the results.

High content screenings are a vital process in drug discovery to rapidly identify potential candidates and pathways to achieve the desired therapeutic benefits. The use of cells comparable to the cellular targets in vivo is

likely to increase the chance of success when moving a drug to pre-clinical and clinical settings. For this reason, cortical neuron screens are commonly used for finding novel therapeutics to increase axon regenerative capacity for neurotraumatic injuries^{76,77}. Considering the many epigenetic^{78,79} and metabolic²¹ changes occurring in neurons as they age, the age-factor should be considered during screenings. For example, pro-inflammatory cytokines deemed harmful to adults are beneficial for the development of young neurons²⁵ and changes in mitochondrial functions impact SCI in an age-dependent manner⁸⁰. Therefore, compounds that modulate cytokine production or mitochondrial functions may produce age-dependent effects⁸⁰. 7-epi Paclitaxel is an example of such a phenomenon for the need to use demographic specific screens. Nonetheless, screening adult, even young adult, neurons has previously not been plausible. Additionally, neuronal cultures are usually grown using growth factors (BDNF, NGF, or NT3)^{21,50,54} which are likely to conceal the beneficial effects of tested compounds. Thanks to the advancements made by Miltenyi in neuron dissociation and isolation, small volumes of primary adult neurons can be cultured^{21,57}. We extensively modified this protocol to mass process larger volumes of cortical tissue with improved methods that reduce costs, increase processing speed, increase total number of cells per preparation, and increase yield and purity (based on qRT-PCR) to conduct screenings using neurons of all ages given enough brain tissue matter.

The MetaXpress[®] 6 automated analysis system from Molecular Devices provides an unbiased analysis at an unprecedented rate allowing for the high content morphology-based neuron screens. The analysis used herein is based on 3 parameters: average neurite length, total neurite outgrowth, and number of valid neurons. First, the software finds nuclei (DAPI) that are associated with neurites (TUBB3). Next, the software determines if the total associated neurites are $\geq 10 \mu\text{m}$ in length and only then considers the cell to be a valid neuron. This analysis method is biased against neurons of very little neurite growth but simultaneously protects the users from falsely accounting debris particles as valid neurons. Notably, using the valid neurons analysis does not allow for the determination of how many neurons survived or how many neurons initiated neurite growth, rather analyzes a combination of the two. Therefore, with this analysis method, we cannot directly conclude that increased valid neurons increases the survival rate, although is hypothesized to be highly associated with the average viability of the entire culture. Next, the software quantifies neurite outgrowth only from these valid neurons and divides that value from the number of valid neurons to determine the average total neurite outgrowth per neuron. To determine the average neurite length, the total neurite outgrowth value is divided by the average number of branches found on only valid neurons. Therefore, the average neurite length analysis cannot determine if the neurites have equal sized branches or very long neurites with minuscule branching neurites. The software cannot specifically analyze the length of the longest neurite which is one factor in determining average neurite length. 7-epi Paclitaxel induces a noticeable increase in the length of the longest neurite (data not included) and significantly increases the average neurite length, therefore, the two analyses can be associated. More laborious analysis methods, such as neurite tracing²¹, can be used to further evaluate morphological changes. Regardless, our analyses provide enough information for determining which compounds have potential in preclinical settings and should be analyzed in further detail before further investment in preclinical trials.

Many variables went into consideration in the formation of the final neuron isolation, processing, and culturing protocol. Deciding the precise details or even inclusion of each step was determined by the effects of that step on each of the variables analyzed and the associated cost, labor, and time requirements. To assess the effects of compounds on neuron morphology, the neuron must be able to survive in culture which requires attaching to the surface and initiating neurite outgrowth and be healthy/viable enough to respond to environmental changes such as the addition of a drug. A protocol that maximizes neuron survival and viability is more versatile to other species, age groups, and regions of the CNS. Our protocol is tailored to cortical neurons, although, with slight modifications, can be used for neurons from other regions. We were able to culture young adult hippocampal and spinal neurons by adding the SM1 supplement in addition to B27⁺ and 10 ng/mL recombinant human brain derived neurotrophic factor (BDNF, Tonbo Biosciences, 21-8366-U010) to the neuron media. BDNF artificially added into culture was expected to increase the viability of neurons plated at low densities, although this was contrary to our findings. BDNF has been found to stop enhancing the survival of hippocampal neurons at ages above E17⁸¹ even though tyrosine receptor kinase B (TrkB), the high-affinity receptor for BDNF, is present in the cortex of adult rodents⁸². It is plausible that B27⁺ contains factors that activate TrkB, therefore, the addition of more BDNF has residual effect. Increasing the concentration of debris removal solution from the recommended 22.5% to $\geq 25\%$ reduces the number of valid neurons tremendously. Conversely, tissue samples containing large amounts of debris prevent the visualization and quantification of neurons and neurites. Although the removal of debris can enhance neuron survival and neurite outgrowth^{83,84}, the debris removal solution may remove essential factors and biological agents that support survival and neurogenesis. In fact, we observed improvements in survival when removing the debris removal step (not shown). However, this is accompanied with a lot of debris that make semi-automatic quantifications difficult. Since the purpose of the assay is to evaluate increases in neurite outgrowth, the protocol is designed to ensure minimal baseline increase in neurite outgrowth without affecting the number of valid neurons. To reduce potential off-target effects, cost, and time, the protocol minimizes reagent usage. Laminin coating was deemed unnecessary and excluded from the protocol (Fig. 1) and the lowest concentration of papain with maximal effect is recommended (Fig. 1). In terms of deciding between neural supplements, B27⁺ significantly improves all 3 variables compared to SM1 and NeuroBrew. The potential problem with using the best supplement such as B27⁺ is it may mask the true effects of compounds by providing an overabundance of growth factors and nutrients. This theory was disproven by the significant effects seen with different drug treatments in culture supplemented with B27⁺ (Figs. 6, 7). Increasing the number of neurons through proper media supplementation allows for larger screens. B27⁺ provides a nice compromise between survival and neurite growth, with a well characterized fetal bovine serum (FBS) free composition, allowing for accurate assessment of the effects of compounds on adult neurons.

The cell plating density is an important aspect of cell cultures⁸⁵ and can dictate the survival of neurons^{52,86}. For hippocampal neurons, cell plating density influences synapse formation⁸⁷, maturation, and intensity of electrical activity⁸⁸. Our data demonstrates the effects of plating density on viability and morphology. At densities < 5000 cells/well, the neurons are less likely to produce the typical elongated neurites characteristic of a healthy neuron and typically too few neurons to accurately determine differences between treatment groups; variability between treatment groups is inversely proportional to the number of neurons quantified. Adult neurons plated at $\geq 15,000$ cells/well have extended and overlapping neurite outgrowth that makes accurate quantification difficult. Having a plating density that is too high ($\geq 15,000$ cells/well) also leads to an overpopulated culture that grows at an expedited rate which can mask the effects of compounds. Therefore, subsequent experiments and the preferred plating density is 10,000 cells for a well with an area of 0.056 cm². As we increased plating density, we observed an exponential increase in number of valid neurons and there is a significant correlation between neurite outgrowth and plating density. Therefore, extrinsic factors associated with plating density may influence both the number of valid neurons and neurite morphology. One potential factor is glutamine released by neighboring neurons⁸⁹. Glutamine is artificially added to the culture media at a final concentration of 2 mM to increase neuron viability yet may not be enough or may only be one of the factors associated with both viability and plating density. Our improved protocol increases the neuron enrichment, as shown by qRT-PCR. However, other neural cells in culture, even if in low abundance, may also influence the density associated effects. Astrocytes release neurotrophic factors, such as BDNF, that augment neuron survival and function⁹⁰. Endothelial cells may also be present in our culture, as we do not remove them with our protocol. These cells can secrete several factors, including GDNF, that can increase neuron survival and neurite growth^{91,92}. While further elucidation is required to determine which organic molecules are released and by which cells, our data identified an appropriate cell density that allows to screen for compounds modulating neuron survival and neurite growth.

Laminin is a glycoprotein that is part of the extracellular matrix and is involved in cell differentiation, attachment, and growth⁹³, partially through its interaction with integrins⁹⁴. Laminin is commonly used as a precoating substrate to assist in the attachment of neurons and can increase the survival and growth of human pluripotent stem cell-derived neurons⁹⁵. The addition of an extra layer of laminin coating on top of the PDL substrate further enhances attachment, survival, and growth of neural precursor cells⁹⁶. Therefore, the addition of a laminin coating was tested on adult neurons with and without B27⁺ to assess its effects on cell attachment and growth. To our surprise, laminin did not impact neurite morphology, or the number of valid neurons and effects were not masked by B27⁺ supplementation. Therefore, the isolated adult cortical neurons do not seem receptive to laminin. We specifically used mouse derived laminin for this experiment to reduce the potential for inflammatory reactions and nonhomology between other species. We hypothesize that adult neurons have a reduced number of integrin receptors, or that downstream pathways are activated to a lesser extent relative to younger neurons resulting in reduced response to laminin coatings. Dorsal root ganglia neurons from P0 rats are able to increase integrin expression in culture while adult neurons are incapable of this adaptation resulting in reduced survival and neurite outgrowth⁹⁷. Transgenic expression of integrins in adult neurons restores their neurite regenerating capacity⁹⁸. Therefore, integrin-dependent substrates, such as laminin, are not necessary to culture adult neurons for short period of time. This observation is in fact of high interest, as it reduces both the cost and time of screening, while minimizing the number of confounding variables. Indeed, not using laminin coatings will allow for screening molecules activating the downstream molecular signaling pathways without potential confounding factors.

The dissociation of neurons from the extracellular matrix is an essential part of neuron isolation. Traditional methods include incubating the brain tissue in digestive enzymes⁹⁹, digesting through mechanical means¹⁰⁰, or both¹⁰¹. To maximize neuronal yield, we opted for using both methods. Papain, which has been used in previous studies to dissociate neurons¹⁰², produced the highest number of valid neurons when used at concentrations ≥ 0.3 mg/mL. It is unknown if papain increases the enzymatic dissociation of neurons from the extracellular matrix or if it is gentler on adult neurons resulting in higher rates of survival compared to other dissociation enzymes. Different incubation times, temperatures, and mechanical dissociation methods were also tested to maximize the number of valid neurons. Lower temperatures and incubation times from Miltenyi's original protocol⁵⁹ were assessed to determine if milder conditions would increase neuron viability and survival. With the use of papain specifically, the reduction in temperature and time yielded significantly less valid neurons hypothesized to be from reduced enzyme efficiency as it is unconceivable how decreasing the temperature and incubation period would reduce the viability of neurons. A very large improvement to traditional methods was achieved with the gentleMACS™ Octo Dissociator with Heaters even when comparing to other methods of agitation. When no agitation method was used, the number of valid neurons were further reduced (data not included). It is unknown why the agitation induced by the gentleMACS™ Octo Dissociator with Heaters cannot be easily replicated using other methods. It may be providing the most effective amount of agitation while other methods may be over or under agitating the brain tissue. Some dissociation protocols require trituration, which are prone to bring great batch to batch variability¹⁰³. Our protocol aims to maximize rigor and reducibility to be more sensitive to effect sizes. Through extensive testing, Miltenyi's original dissociation method is the best tested method to increase the number of valid adult neurons. Figure 1 demonstrates the effects the dissociation enzymes have on the viability and growth capacity of neurons. The images also demonstrate that papain increases neuronal purity. RT-qPCR based RNA expression analysis confirmed the modified protocol (using papain instead of P&A) has higher neuronal yield and purity relative to Miltenyi's original protocol which concurs with the images; automated morphology analysis only confirmed greater number of valid neurons as the other variables were not analyzed (Fig. 1A–C). However, we did not conduct RNA expression analysis directly comparing the effects of substituting P&A with papain on neuronal yield and purity. Further experimentation is required to elucidate the effects of various dissociation enzymes on neuron health.

Many potent compounds are hydrophobic and require the use of special solvents, which can be harmful to neurons. DMSO is a class 3 solvent (Food and Drug Administration) used to increase the solubility of hydrophobic compounds⁵⁷. Therefore, many high content screens utilize DMSO to dissolve and prevent precipitation of hydrophobic compounds in cell culture media^{68,69}. The issue of using DMSO as a vehicle is its toxicity to neurons and can alter their properties. A brief treatment of 0.05% DMSO induces neurophysiological changes to both hippocampal and cortical neurons¹⁰⁴. DMSO concentrations $\geq 0.5\%$ induce neurite retraction of primary embryonic neurons¹⁰⁵. The effects of DMSO on adult cortical neurons have not been assessed before, and it is necessary to determine the best concentration minimizing the impact of DMSO on neurons while being high enough to allow the solubilization of most compounds tested in future screens. Based on our findings, it is recommended that the use of DMSO in high content screenings in adult neurons follow 2 criteria: (1) The use of DMSO is minimized and is $\leq 0.05\%$ of the culture media; (2) the concentration of DMSO is kept consistent between all cohorts to reduce the confounding effect of DMSO on the analysis. The mechanism of such outcomes has yet to be elucidated. One possibility is the reduction of ERK phosphorylation. Indeed, phosphorylation of ERK, induced by alpha-lipoic acid in mouse neuroblastoma N2a cells, promotes neurite outgrowth¹⁰⁶, while DMSO has been shown to reduce ERK phosphorylation in blood cells¹⁰⁷. Therefore, DMSO may be reducing the neurite outgrowth potential of neurons by modulating the ERK pathway. DMSO also reduces the number of valid neurons (total neurite outgrowth of $\geq 10 \mu\text{m}$) in a dose-dependent manner which is associated with a reduction in neurite outgrowth (Fig. 5). Therefore, it is plausible the reduction in neurite outgrowth is merely from the reduction in neuron survival. The sensitivity of adult neurons to DMSO results in screening limitations, therefore, other solvents should be considered for testing compounds at higher concentrations.

Due to the vast range of responses the general population has towards a given therapeutic^{108,109}, it is vital to consider the age and sex factor in the development of new therapeutics. The cells isolated from that demographic are expected to respond differently as well. Here, we determined the demographic specific effects of RO48 and 7-epi Paclitaxel in our targeted screen to demonstrate the necessity for conducting demographic specific screens in neurons to ensure the compounds influence the target audience. Our *in vitro* cell cultures have identical conditions between age groups and are from very genetically similar mice. Thus, cell cultures allow us to determine how the neuron's sex chromosomes (sex difference) or epigenetic profile (age-dependent effect) impact neuronal phenotype without known confounding variables. Through our specific processing and culturing methodology, we discovered both sex and age differences in response to exposure to different drugs.

We demonstrated that RO48 induces both sex- and age-dependent effects on neuron morphology and viability. RO48 activates mTORC1/2 and PI3K and decreases the phosphorylation of S6-926⁷⁰ and S6K1 which are negative regulators of neurite growth¹¹⁰. Overall, RO48 present positive effects regardless of sex and age. RO48 significantly increases the average of neurite length in young adult neurons and increases the total neurite outgrowth only in older females. RO48 is very effective at increasing the number of valid neurons, which is expected since both mTOR and S6K1 increase neuron survival¹¹¹. Intriguingly, the potency of RO48 to increase the number of valid neurons differs significantly with age and sex. One explanation for the smaller effect of RO48 at increasing the number of valid neurons with age is the age-dependent reduction in mitochondrial function. Indeed, S6K1 enhances mitochondrial ATP production¹¹² which is important for axon growth and cell survival and could be a mechanism of action of RO48. However, we recently demonstrated that aging reduces neuronal mitochondrial capacity and efficiency²¹. Therefore, it is possible that the increase in ATP production in presence of RO48 is not as potent in older neurons, leading to a reduced activity of RO48. PI3K may also be involved in the age-dependent effects. PI3K decreases as cells age¹¹³. PI3K reduces neurite branch formation¹¹⁴ which would lead to an increase in the average neurite length. Since only the younger cohorts have increased neurite length in response to RO48, there may be an age-dependent response to PI3K modulation or age-dependent ability to express PI3K resulting in the significant differences in average neurite length in response to RO48. The single instance RO48 was not beneficial was in the average neurite length on middle-aged female neurons. There is a decrease in the ratio of phosphorylated mTOR in middle-aged naked mole rats compared to their young adult counterparts¹¹⁵ which is part of the mTOR activation process¹¹⁶. The mTOR pathway is an essential part of neurite formation^{117–119}. Since there was a significantly greater increase in total neurite outgrowth in the older cohort in response to RO48 relative to their younger counterparts, and a greater increase in average neurite length in younger cohorts relative to the middle-aged female cohort, it may be plausible that mTOR phosphorylation induces neurite growth in all cohorts in a similar manner. The differences between age groups may be due to the management of neurite elongation. Indeed, we have shown at 7DIV, neurons from aged mice have more branching²¹. This may be due to neurons from younger mice better consolidating and focusing neurite growth into few branches for the objective of producing axons. Nonetheless, direct experimentation is required to elucidate the pathways responsible these differences.

The sex differences of RO48 might be due to the activation of sex-dependent pathways. PI3K inhibition increases hepatic GSH content, antioxidant genes, and catalase in males but not in females¹²⁰. The increase of catalase activity is correlated with reduction in neurite outgrowth¹²¹, therefore, one intriguing possibility is that the influence of PI3K on neurite outgrowth is sex-dependent. Another possibility is the S6 phosphorylation rate difference. Indeed, female mice have significantly higher rates of S6 phosphorylation in both the liver and heart¹²², and therefore, may be more susceptible to the reduction in S6 phosphorylation induced by RO48⁷⁰. This remains to be determined in cortical neurons. Inhibition of mTOR only increases brain proteasome activity in females¹²³. Proteasome inhibition is a potential therapeutic option for increasing neurite outgrowth¹²⁴, therefore, sex differences in neurite outgrowth through the mTOR-proteasome pathway would not be surprising.

7-epi Paclitaxel is an FDA-approved drug for use in patients with ovarian cancer⁷². 7-epi Paclitaxel stabilizes microtubule bundles, impairs organelle transport⁷³, and induces peripheral neuropathy through the CXCR1/2 pathway⁷⁴. 7-epi Paclitaxel improved the average neurite length of all 3 demographics tested yet was toxic only to young adults demonstrated by reduced neurite outgrowth and number of valid neurons. However, severe

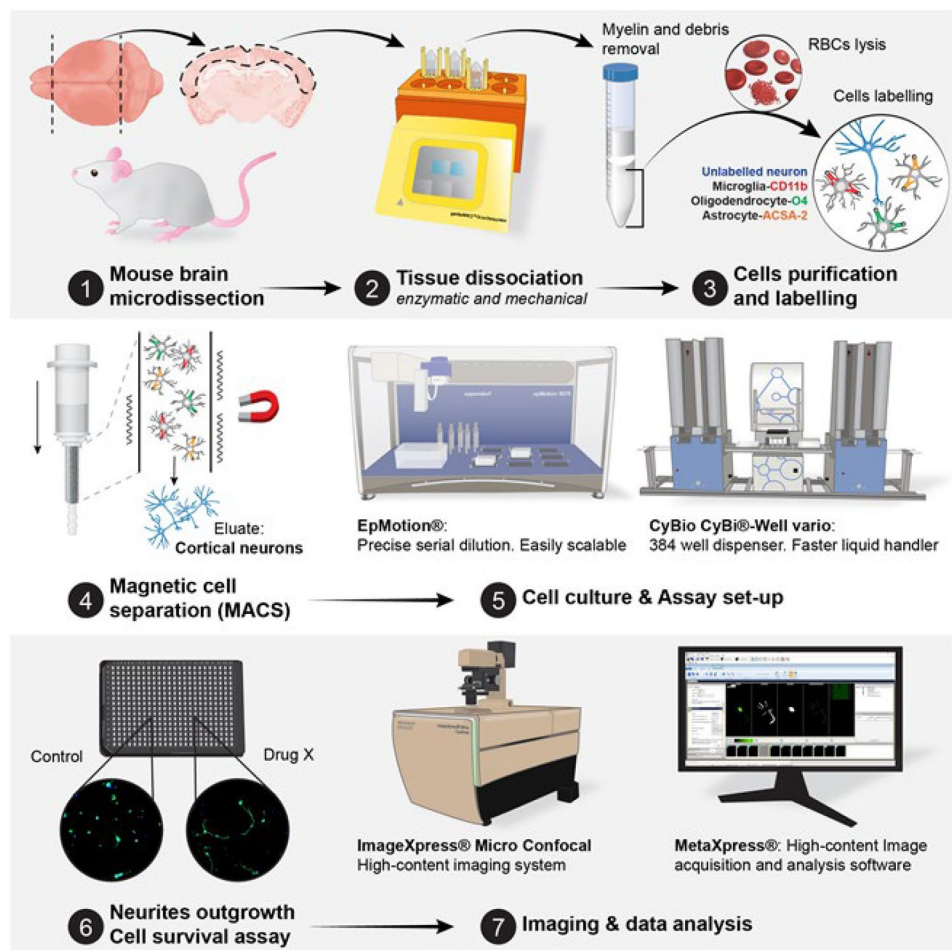


Figure 8. The screening platform using primary adult neural cells. Briefly, the cortex is extracted from mice, dissociated in a dissociator, followed by the removal of debris and red blood cells. Afterwards, the glial cells are separated from neurons. All liquid handling, imaging, and analysis is done with bias and human free robots. Figure was created by Graphit Science & Art, LLC.

neurotoxicity occurs sooner and more frequently in older metastatic breast cancer patients treated with 7-epi Paclitaxel compared to younger patients¹²⁵. This discrepancy may be due to older patients generally being more vulnerable to neurotoxicity regardless of the treatment^{126,127}. Conceivably, the increased 7-epi Paclitaxel-induced toxicity in older patients may be due to pharmacokinetic changes in aged patients that lead to prolonged drug activity and toxicity and increased drug sensitivity¹²⁸. Therefore, it is plausible 7-epi Paclitaxel is less toxic to older neurons yet still more toxic to older patients. Interestingly, the CXCR1/2 expression is increased with age in rat cortical neurons¹²⁹. The lower baseline of CXCR1/2 levels in younger neurons may explain the increased neurotoxicity relative to middle-aged neurons. Further direct experimentation is required to elucidate the age-dependent neurotoxicity of 7-epi Paclitaxel.

Conclusion

Screening for compounds directly in adult cortical neurons has been so far unrealistic. Here, we established a new protocol that augments our ability to screen directly in primary mouse adult cortical neurons (Fig. 8). We conducted targeted screenings and demonstrated both age- and sex-dependent effects of multiple compounds. We established that: (1) dosage can intrinsically be sex-dependent; (2) screening in younger demographics will cause premature dismissal of compounds beneficial to older demographics; and (3) aging alters neuronal characteristics and therefore, must be considered in future screenings, especially for age-associated neurological disorders. This novel methodology is expected to strengthen the drug discovery process for neurological disorders and neurotraumatic injuries by providing more relevant *in vitro* data increasing the likelihood of preclinical and clinical success.

Methods

Animals. This study uses young adult and middle-aged male and female wild-type C57Bl/6 mice. The young adult group is of 4–9 weeks of age and the middle-age group is of 40–48 weeks of age. All procedures were conducted according to the protocol approved by the Institutional Review Board/Animal Ethics Committee of Texas A&M University (IACUC 2018-0324).

Cell culture. The following is the final protocol after the completion of optimizations. First, 20 μL of 50 $\mu\text{g}/\text{mL}$ Poly-D-Lysine (PDL, Sigma Aldrich, A-003-M) was added onto the wells of 384-well glass bottom (Brooks Life Sciences, MGB101-1-2-LG-L) or plastic bottom (Greiner-Bio, 781091) plates and incubated inside a 5% CO_2 incubator at 37 $^\circ\text{C}$ for 48 h. In instances laminin was used, laminin was added at a concentration of 10 $\mu\text{g}/\text{mL}$ and incubated at 37 $^\circ\text{C}$ for 1 h before being washed once immediately before cell plating. After incubation, the wells of the plates were washed 5 times with H_2O and set to dry overnight at room temperature and were used within 24 h after drying. After euthanization of mice, the brains were extracted and placed in cold Hank's balanced salt solution (HBSS) followed by microdissection of the cortex. Up to 1.25 g of cortical tissue were placed in each gentleMACS™ C Tube (Miltenyi Biotec, # 130-093-237) which contained 5 mL of 0.3 mg/mL papain (Worthington, LS003126) diluted in HBSS. The gentleMACS™ C Tubes were placed on the gentleMACS™ Octo Dissociator with Heaters (Miltenyi Biotec, # 130-096-427) with heating cuffs attached and underwent the gentleMACS Program 37C_ABDK_01 protocol. After protocol completion, the contents of the gentleMACS™ C Tube were strained through a 70 μm cell strainer (Miltenyi Biotec, # 130-110-916) placed on top of a 15 mL conical centrifuge tube. 7 mL of cold Dulbecco's Phosphate-Buffered Saline with glucose and pyruvate (DPBS, Thermo Fisher Scientific, 14287072) was added into each of the 15 mL conical centrifuge tubes on top of the strained cells. The 15 mL tubes were centrifuged at 300 $\times g$ for 10 min at 4 $^\circ\text{C}$ before aspirating the supernatant completely. Debris removal solution was made by adding 1800 μL of Debris Removal Concentrate (Miltenyi Biotec, # 130-109-398) to 6200 μL of cold DPBS. The remaining pellet inside the 15 mL tubes was resuspended with 8 mL of Debris Removal Solution. Very slowly, 4 mL of cold DPBS was dispensed on top of the debris removal solution and cell mixture in each 15 mL tube forming a clear layer on top. The 15 mL tubes were centrifuged at 3000 $\times g$ for 10 min at 4 $^\circ\text{C}$ with slow acceleration and deceleration. The top clear and middle debris layers were aspirated leaving the milky mixture beneath the debris layer untouched. 6 mL of DPBS was added onto the milky mixture and mixed gently before centrifuging at 300 $\times g$ for 5 min at 4 $^\circ\text{C}$. All supernatant was aspirated afterwards. Red Blood Cell Remover Solution was made by mixing 125 μL of Red Blood Cell Lysis Solution 10 \times (Miltenyi Biotec, # 130-094-183) with 1125 μL of H_2O . The remaining pellet was resuspended in 1.25 mL of Red Blood Cell Remover Solution and incubated for 10 min at 4 $^\circ\text{C}$ before the addition of 12 mL of 0.5% bovine serum albumin (BSA, Miltenyi Biotec, # 130-091-376) diluted in DPBS. The mixture was centrifuged at 300 $\times g$ for 5 min at 4 $^\circ\text{C}$ with the supernatant aspirated completely afterwards. The remaining pellet was resuspended in 80 μL of 0.5% BSA and 20 μL of Non-Neuronal Cells Biotin-Antibody Cocktail (Miltenyi Biotec, # 130-115-389) and incubated for 5 min at 4 $^\circ\text{C}$. Cells were washed by adding 2 mL of 0.5% BSA followed by centrifugation at 300 $\times g$ for 5 min at 4 $^\circ\text{C}$ followed by aspiration of the supernatant. The remaining pellet was resuspended in 80 μL of 0.5% BSA and 20 μL of Anti-Biotin MicroBeads (Miltenyi Biotec, # 130-115-389) and incubated for 10 min at 4 $^\circ\text{C}$. After the addition of 6 mL 0.5% BSA, the mixture was flowed through 0.5% BSA primed LS columns (Miltenyi Biotec, #130-042-401). The negative fraction containing the majority of neurons was collected and centrifuged at 300 $\times g$ for 5 min at 4 $^\circ\text{C}$ and resuspended in neuron media. Unless noted otherwise, neuron media consists of MACS Neuro Media (Miltenyi Biotec, # 130-093-570), 2 mM L-alanine-L-glutamine dipeptide (Sigma-Aldrich, G8541-100ML), and 1 \times B-27™ Plus Supplement (ThermoFisher Scientific, A3582801). We followed the respective instruction manuals for all neuronal supplement use (B27⁺, SM1, NeuroBrew). All supplements came in a 50 \times solution and were diluted to a final concentration of 1 \times following manufacturer's instructions. Unless noted otherwise, cells were added onto PDL coated wells and placed inside a 5% CO_2 incubator set at 37 $^\circ\text{C}$ for the stated days in vitro (DIV). Unless noted otherwise, 10,000 cells were plated per well with 0.056 cm^2 growth area. The neuron isolation, processing, and plating procedure described herein is referred to as the 'Modified Protocol'.

RT-qPCR for determining cell culture purity. RT-qPCR assay was replicated as previously described²¹. Briefly, the cells isolated from cortical tissue of young adult male mice were pelleted after the completion of the respective protocol followed by the extraction of RNA immediately after. Directzol RNA micro-prep columns (Zymo, R2061) are used to extract RNA from neurons directly following neuron isolation. RNA concentration was measured using the Thermo Scientific™ NanoDrop 2000. Quantabio cDNA Synthesis kit (Quanta, 95047) was used to synthesize cDNA before conducting qPCR using the Quantabio PerfeCTa™ SYBR™ Green FastMix™ (Quanta, 95073) on the ViiA7 Real Time PCR system (Life Technologies). The neuron enrichment in the negative fraction was calculated as previously described²¹, $-\Delta\text{CT}$ of ΔNeuN against ΔGFAP and ΔGLAST using the formula: $-\Delta\text{CT} = -(\Delta\text{CT}_{\text{NeuN}} - (\text{SQRT}(\Delta\text{CT}_{\text{GFAP}^2} + \Delta\text{CT}_{\text{GLAST}^2})))$. CT was calculated for each group based on the absolute CT per primer subtracted by the respective CT of the negative control to reduce background noise. For each group, RNA was extracted from 3 separate isolation procedures from young adult males and each sample was analyzed in triplicate. β -actin was used as the internal housekeeping gene control to normalize gene expression. No outliers were detected nor omitted.

Primers used to identify the main cellular constituents

Neurons *MAP2* (F: 5'-CTG GAG GTG GTA ATG TGA AGA TTG; R: 5'-TCT CAG CCC CGT GAT CTA CC-3') and *NeuN* (F: 5'-AAC CAG CAA CTC CACCCT TC-3'; R: 5'-CGA ATT GCC CGA ACA TTT GC-3'). Astrocytes: *GFAP* (F: 5'-CTA ACG ACT ATC GCC GCC AA-3'; R: 5'-CAG GAA TGG TGA TGC GGT TT-3') and *GLAST* (F: 5'-CAA CGA AAC ACT TCT GGG CG-3'; R: 5'-CCA GAG GCG CAT ACC ACA TT-3').

Oligodendrocytes: *Oligo2* (F: 5'- GAA CCC CGA AAG GTG TGG AT-3'; R: 5'-TTC CGA ATG TGA ATT AGA TTT GAG G-3'). β -*actin*: (F: 5'-CTC TGG CTC CTA GCA CCA TGA AGA-3'; R: 5'-GTA AAA CGC AGC TCA GTA ACA GTC CG-3').

Immunocytochemistry. Cell cultures were fixed with 4% paraformaldehyde (PFA, 15 min) after the completion of the respective experiment. After fixation, immunocytochemistry was conducted by first washing the cells with DPBS 3 times, then incubating in 5% normal horse serum for 60 min to block nonspecific binding (VWR, 102643-676). Afterwards, the cells were incubated in 1:500 TUBB3 (BioLegend, 801202) for 16 h, followed by another 3 washes with DPBS and incubation in 1:500 Alexa Fluor 488 (ThermoFisher Scientific, A32723) and 1:10,000 DAPI (VWR, 95059-474) for 60 min, all conducted at room temperature. After the completion of immunocytochemistry, the cells were preserved in Fluoromount-G Mounting Medium (ThermoFisher Scientific, 00-4958-02) until imaging. All experimentation after incubation in secondary antibody was performed in the absence of light.

Analysis of neurite outgrowth and survival. Representative images in figures were imaged using 20 \times /63 \times objectives on a Zeiss Axio Observer system. For automated image acquisition, the \times 20 magnification lens of the ImageXpress (IXM) Micro Confocal High-Content Imaging System (Molecular Devices, San Jose, CA) was used along with the Neurite Outgrowth Analysis Module in MetaXpress[®] 6 software (Molecular Devices) for automated image analysis, a system previously used to image and analyze changes in neuron morphology^{28,130–132}. Using the \times 20 magnification, 16 separate images (with 10% overlap) were required to sustain >90% coverage of each well while avoiding the walls.

Three variables were quantified.

1. *Valid neurons* Total number of cells in a well that are both DAPI and TUBB3 positive and with total neurite outgrowth of $\geq 10 \mu\text{m}$.
2. *Total neurite outgrowth* Sum of the lengths of all the neurites from a valid neuron. This is then averaged over all the valid neurons in a well.
3. *Average neurite length* The total length of all the neurites from a valid neuron divided by the number of neurites and branches of that cell. This is then averaged over all the valid neurons in the well.

Data analysis. Normally distributed data was analyzed using unpaired t-test when comparing 2 means and one-way analysis of variance (ANOVA) with Tukey's or Dunnett's post-hoc test when comparing >2 means. Tukey's post-hoc test is used to compare >2 means all with one another. Dunnett's post-hoc test is used to compare ≥ 2 means to the mean of a particular group. Two-way ANOVA was used to analyze the effects of 2 independent variables on the expected outcome. Tukey's multiple comparisons test was used to compare the means of each cohort with the means of all other cohorts. Dunnett's multiple comparisons test was used to compare the means of each cohort to the mean of a particular cohort. Šidák's multiple comparisons test was used to compare the means of 2 independent groups for all cohorts. Simple linear regression was conducted to determine goodness of fit (R^2) and to determine the correlation between 2 independent variables. Linear regression t-test was used to compare the slopes of 2 independent regression lines. Analysis and graphing were conducted using Graphpad Prism 9. All graphs represent the data mean with error bars illustrating the standard error of the mean (SEM).

Compounds. RO48 (generously provided by Drs. Lemmon, Bixby, and Al-Ali from Miami Project to Cure Paralysis, University of Miami), (S)-H-1152 (Cayman Chemical Company, 10007653), and 7-epi Paclitaxel (Cayman Chemical Company, 20741). All compounds are added to the media at the time of cell plating. No media changes occur during the entire duration of the assay; therefore, the cells are incubated with the compounds for the entire duration of the assay.

Institutional review board statement. The study was conducted and approved by the Institutional Animal Care Committee at Texas A&M University (IACUC 2018-0048). All the experiments reported here were reviewed and approved by the and were consistent with the ARRIVE guidelines for animal care and use. All methods were carried out in accordance with the guidelines and regulations from the Institutional Biosafety Committee at Texas A&M (IBC-2018-011).

Data availability

The authors confirm that the data supporting the findings of this study are available within the article or its Supplementary Materials.

Received: 18 April 2022; Accepted: 25 July 2022

Published online: 30 July 2022

References

1. Kanasi, E., Ayilavarapu, S. & Jones, J. The aging population: Demographics and the biology of aging. *Periodontol 2000* **72**, 13–18. <https://doi.org/10.1111/prd.12126> (2016).
2. Riggs, J. E. The aging population: Implications for the burden of neurologic disease. *Neurol. Clin.* **16**, 555–560. [https://doi.org/10.1016/S0733-8619\(05\)70079-7](https://doi.org/10.1016/S0733-8619(05)70079-7) (1998).
3. Statista. (Statista, statista.com, 2021).

4. Murray, C. J. L. *et al.* Disability-adjusted life years (DALYs) for 291 diseases and injuries in 21 regions, 1990–2010: A systematic analysis for the Global Burden of Disease Study 2010. *The Lancet* **380**, 2197–2223. [https://doi.org/10.1016/S0140-6736\(12\)61689-4](https://doi.org/10.1016/S0140-6736(12)61689-4) (2012).
5. Centers for Disease Control and Prevention. *Rates of TBI-related Hospitalizations by Age Group—United States, 2001–2010*, https://www.cdc.gov/traumaticbraininjury/data/rates_hosp_byage.html Accessed 21 July 2022 (2016).
6. Fassett, D. R. *et al.* Mortality rates in geriatric patients with spinal cord injuries. *J. Neurosurg. Spine* **7**, 277–281. <https://doi.org/10.3171/spi-07/09/277> (2007).
7. Chi, H., Chang, H.-Y. & Sang, T.-K. Neuronal cell death mechanisms in major neurodegenerative diseases. *Int. J. Mol. Sci.* **19**, 3082. <https://doi.org/10.3390/ijms19103082> (2018).
8. Romaus-Sanjurjo, D. *et al.* GABA promotes survival and axonal regeneration in identifiable descending neurons after spinal cord injury in larval lampreys. *Cell Death Dis.* **9**, 663. <https://doi.org/10.1038/s41419-018-0704-9> (2018).
9. da Silva Meirelles, L., Simon, D. & Regner, A. Neurotrauma: The crosstalk between neurotrophins and inflammation in the acutely injured brain. *Int. J. Mol. Sci.* **18**, 1082. <https://doi.org/10.3390/ijms18051082> (2017).
10. Steward, M. M., Sridhar, A. & Meyer, J. S. Neural regeneration. *Curr. Top. Microbiol. Immunol.* **367**, 163–191. https://doi.org/10.1007/82_2012_302 (2013).
11. Grossman, R. G. (clinicaltrials.gov, 2010).
12. Farhadi, H. F. (clinicaltrials.gov, 2017).
13. Casha, S. (clinicaltrials.gov, 2004).
14. Ulndrea, A., Badner, A. & Fehlings, M. G. Promising neuroprotective strategies for traumatic spinal cord injury with a focus on the differential effects among anatomical levels of injury. *F1000Research* **6**, 1907–1907. <https://doi.org/10.12688/f1000research.11633.1> (2017).
15. Longo, F. M. & Massa, S. M. Neuroprotective strategies in Alzheimer’s disease. *NeuroRx J. Am. Soc. Exp. Neurotherap.* **1**, 117–127. <https://doi.org/10.1602/neurorx.1.1.117> (2004).
16. Ueno, M. & Yamashita, T. Strategies for regenerating injured axons after spinal cord injury—Insights from brain development. *Biol. Targets Therapy* **2**, 253–264. <https://doi.org/10.2147/btt.s2715> (2008).
17. Geoffroy, C. G. *et al.* Effects of PTEN and nogo codeletion on corticospinal axon sprouting and regeneration in mice. *J. Neurosci.* **35**, 6413–6428. <https://doi.org/10.1523/jneurosci.4013-14.2015> (2015).
18. Lingor, P., Koch, J. C., Tönges, L. & Bähr, M. Axonal degeneration as a therapeutic target in the CNS. *Cell Tissue Res.* **349**, 289–311. <https://doi.org/10.1007/s00441-012-1362-3> (2012).
19. Welsbie, D. S. *et al.* Functional genomic screening identifies dual leucine zipper kinase as a key mediator of retinal ganglion cell death. *Proc. Natl. Acad. Sci. U.S.A.* **110**, 4045–4050. <https://doi.org/10.1073/pnas.1211284110> (2013).
20. Qian, C. & Zhou, F.-Q. Updates and challenges of axon regeneration in the mammalian central nervous system. *J. Mol. Cell Biol.* **12**, 798–806. <https://doi.org/10.1093/jmcb/mjaa026> (2020).
21. Sutherland, T. C. *et al.* Age-dependent decline in neuron growth potential and mitochondria functions in cortical neurons. *Cells* **10**, 1625 (2021).
22. Mattson, M. P. & Magnus, T. Ageing and neuronal vulnerability. *Nat. Rev. Neurosci.* **7**, 278–294. <https://doi.org/10.1038/nrn1886> (2006).
23. Hukkelhoven, C. W. *et al.* Patient age and outcome following severe traumatic brain injury: An analysis of 5600 patients. *J. Neurosurg.* **99**, 666–673. <https://doi.org/10.3171/jns.2003.99.4.0666> (2003).
24. Hou, Y. *et al.* Ageing as a risk factor for neurodegenerative disease. *Nat. Rev. Neurol.* **15**, 565–581. <https://doi.org/10.1038/s41582-019-0244-7> (2019).
25. Sefiani, A. & Geoffroy, C. G. The potential role of inflammation in modulating endogenous hippocampal neurogenesis after spinal cord injury. *Front. Neurosci.* <https://doi.org/10.3389/fnins.2021.682259> (2021).
26. Al-Ali, H., Schürer, S. C., Lemmon, V. P. & Bixby, J. L. Chemical interrogation of the neuronal kinome using a primary cell-based screening assay. *ACS Chem. Biol.* **8**, 1027–1036. <https://doi.org/10.1021/cb300584e> (2013).
27. Jiang, H. *et al.* Live neuron high-content screening reveals synaptotoxic activity in alzheimer mouse model homogenates. *Sci. Rep.* **10**, 3412. <https://doi.org/10.1038/s41598-020-60118-y> (2020).
28. Sirenko, O., Hesley, J., Rusyn, I. & Cromwell, E. F. High-content high-throughput assays for characterizing the viability and morphology of human iPSC-derived neuronal cultures. *Assay Drug Dev. Technol.* **12**, 536–547. <https://doi.org/10.1089/adt.2014.592> (2014).
29. Spicer, T. P. *et al.* Improved scalability of neuron-based phenotypic screening assays for therapeutic discovery in neuropsychiatric disorders. *Complex Psychiatry* **3**, 141–150. <https://doi.org/10.1159/000481731> (2017).
30. Varkuti, B. H. *et al.* Neuron-based high-content assay and screen for CNS active mitochondria. *Sci. Adv.* **6**, 8702. <https://doi.org/10.1126/sciadv.aaw8702> (2020).
31. Shirokawa, T., Ishida, Y. & Isobe, K. I. Age-dependent changes in axonal branching of single locus coeruleus neurons projecting to two different terminal fields. *J. Neurophysiol.* **84**, 1120–1122. <https://doi.org/10.1152/jn.2000.84.2.1120> (2000).
32. Geoffroy, C. G., Hilton, B. J., Tetzlaff, W. & Zheng, B. Evidence for an age-dependent decline in axon regeneration in the adult mammalian central nervous system. *Cell Rep.* **15**, 238–246. <https://doi.org/10.1016/j.celrep.2016.03.028> (2016).
33. Dhir, N. *et al.* Pre-clinical to clinical translational failures and current status of clinical trials in stroke therapy: A brief review. *Curr. Neuropharmacol.* **18**, 596–612. <https://doi.org/10.2174/1570159X18666200114160844> (2020).
34. Kelly-Hayes, M. Influence of age and health behaviors on stroke risk: Lessons from longitudinal studies. *J. Am. Geriatr. Soc.* **58**(Suppl 2), S325–S328. <https://doi.org/10.1111/j.1532-5415.2010.02915.x> (2010).
35. Lucke-Wold, B. P., Turner, R. C., Lucke-Wold, A. N., Rosen, C. L. & Huber, J. D. Age and the metabolic syndrome as risk factors for ischemic stroke: Improving preclinical models of ischemic stroke. *Yale J. Biol. Med.* **85**, 523–539 (2012).
36. Saposnik, G. *et al.* Stroke outcome in those over 80: A multicenter cohort study across Canada. *Stroke* **39**, 2310–2317. <https://doi.org/10.1161/strokeaha.107.511402> (2008).
37. Urban, K. R., Waterhouse, B. D. & Gao, W. J. Distinct age-dependent effects of methylphenidate on developing and adult prefrontal neurons. *Biol. Psychiatry* **72**, 880–888. <https://doi.org/10.1016/j.biopsych.2012.04.018> (2012).
38. Anderson, G. D. Gender differences in pharmacological response. *Int. Rev. Neurobiol.* **83**, 1–10. [https://doi.org/10.1016/s0074-7742\(08\)00001-9](https://doi.org/10.1016/s0074-7742(08)00001-9) (2008).
39. Soldin, O. P. & Mattison, D. R. Sex differences in pharmacokinetics and pharmacodynamics. *Clin. Pharmacokinet.* **48**, 143–157. <https://doi.org/10.2165/00003088-200948030-00001> (2009).
40. Whitley, H. & Lindsey, W. Sex-based differences in drug activity. *Am. Fam. Phys.* **80**, 1254–1258 (2009).
41. Equebal, A., Anwer, S. & Kumar, R. The prevalence and impact of age and gender on rehabilitation outcomes in spinal cord injury in India: A retrospective pilot study. *Spinal Cord* **51**, 409–412. <https://doi.org/10.1038/sc.2013.5> (2013).
42. Leppert, M. H. *et al.* Young women had more strokes than young men in a large, United States claims sample. *Stroke* **51**, 3352–3355. <https://doi.org/10.1161/strokeaha.120.030803> (2020).
43. Handelsman, D. J. Sex differences in athletic performance emerge coinciding with the onset of male puberty. *Clin. Endocrinol. (Oxf.)* **87**, 68–72. <https://doi.org/10.1111/cen.13350> (2017).
44. Paus, T., Wong, A. P., Syme, C. & Pausova, Z. Sex differences in the adolescent brain and body: Findings from the saguenay youth study. *J. Neurosci. Res.* **95**, 362–370. <https://doi.org/10.1002/jnr.23825> (2017).

45. Zhang, Q., Zeng, Y., Zhang, T. & Yang, T. Comparison between human and rodent neurons for persistent activity performance: A biologically plausible computational investigation. *Front. Syst. Neurosci.* **15**, 628839–628839. <https://doi.org/10.3389/fnsys.2021.628839> (2021).
46. Silva, M. C. & Haggarty, S. J. Human pluripotent stem cell-derived models and drug screening in CNS precision medicine. *Ann. N. Y. Acad. Sci.* **1471**, 18–56. <https://doi.org/10.1111/nyas.14012> (2020).
47. Farkhondeh, A. *et al.* Induced pluripotent stem cells for neural drug discovery. *Drug Discov. Today* **24**, 992–999. <https://doi.org/10.1016/j.drudis.2019.01.007> (2019).
48. Yun, M. H. Changes in regenerative capacity through lifespan. *Int. J. Mol. Sci.* **16**, 25392–25432. <https://doi.org/10.3390/ijms161025392> (2015).
49. Du, X. & Parent, J. M. Using patient-derived induced pluripotent stem cells to model and treat epilepsies. *Curr. Neurol. Neurosci. Rep.* **15**, 71–71. <https://doi.org/10.1007/s11910-015-0588-3> (2015).
50. Park, T. I. H. *et al.* Isolation and culture of functional adult human neurons from neurosurgical brain specimens. *Brain Commun.* **2**, 171. <https://doi.org/10.1093/braincomms/fcaa171> (2020).
51. Carlson, M. E. & Conboy, I. M. Loss of stem cell regenerative capacity within aged niches. *Aging Cell* **6**, 371–382. <https://doi.org/10.1111/j.1474-9726.2007.00286.x> (2007).
52. Eide, L. & McMurray, C. T. Culture of adult mouse neurons. *Biotechniques* **38**, 99–104. <https://doi.org/10.2144/05381rr02> (2005).
53. Berl, S. *et al.* Enrichment and isolation of neurons from adult mouse brain for ex vivo analysis. *J. Neurosci. Methods* **283**, 15–22. <https://doi.org/10.1016/j.jneumeth.2017.03.015> (2017).
54. Brewer, G. J. & Torricelli, J. R. Isolation and culture of adult neurons and neurospheres. *Nat. Protoc.* **2**, 1490–1498. <https://doi.org/10.1038/nprot.2007.207> (2007).
55. Welzel, G., Seitz, D. & Schuster, S. Magnetic-activated cell sorting (MACS) can be used as a large-scale method for establishing zebrafish neuronal cell cultures. *Sci. Rep.* **5**, 7959. <https://doi.org/10.1038/srep07959> (2015).
56. Bohlen, C. J., Bennett, F. C. & Bennett, M. L. Isolation and culture of microglia. *Curr. Protoc. Immunol.* **125**, e70. <https://doi.org/10.1002/cpim.70> (2019).
57. Schroeter, C. B. *et al.* One brain—All cells: A comprehensive protocol to isolate all principal CNS-resident cell types from brain and spinal cord of adult healthy and EAE mice. *Cells* **10**, 651 (2021).
58. Lee, S. K. Sex as an important biological variable in biomedical research. *BMB Rep.* **51**, 167–173. <https://doi.org/10.5483/bmbrep.2018.51.4.034> (2018).
59. Miltenyi Biotec. Adult Brain Dissociation Kit mouse and rat. 140-004-828.05. <https://www.miltenyibiotec.com/upload/assets/IM0011920.PDF> (2020).
60. Clelland, L. J., Browne, B. M., Alvarez, S. M., Miner, A. S. & Ratz, P. H. Rho-kinase inhibition attenuates calcium-induced contraction in β -escin but not Triton X-100 permeabilized rabbit femoral artery. *J. Muscle Res. Cell Motil.* **32**, 77–88. <https://doi.org/10.1007/s10974-011-9253-x> (2011).
61. Fuentes, E. O., Leemhuis, J., Stark, G. B. & Lang, E. M. Rho kinase inhibitors Y27632 and H1152 augment neurite extension in the presence of cultured Schwann cells. *J. Brachial Plexus Peripheral Nerve Inj.* **3**, 19–19. <https://doi.org/10.1186/1749-7221-3-19> (2008).
62. Seilheimer, B., Persohn, E. & Schachner, M. Neural cell adhesion molecule expression is regulated by Schwann cell-neuron interactions in culture. *J. Cell Biol.* **108**, 1909–1915. <https://doi.org/10.1083/jcb.108.5.1909> (1989).
63. Bardy, C. *et al.* Neuronal medium that supports basic synaptic functions and activity of human neurons in vitro. *Proc. Natl. Acad. Sci.* **112**, E2725–E2734. <https://doi.org/10.1073/pnas.1504393112> (2015).
64. Brewer, G. J., Torricelli, J. R., Evege, E. K. & Price, P. J. Optimized survival of hippocampal neurons in B27-supplemented neurobasal, a new serum-free medium combination. *J. Neurosci. Res.* **35**, 567–576. <https://doi.org/10.1002/jnr.490350513> (1993).
65. Zabolocki, M. *et al.* BrainPhys neuronal medium optimized for imaging and optogenetics in vitro. *Nat. Commun.* **11**, 5550–5550. <https://doi.org/10.1038/s41467-020-19275-x> (2020).
66. Chen, Y. *et al.* NS21: Re-defined and modified supplement B27 for neuronal cultures. *J. Neurosci. Methods* **171**, 239–247. <https://doi.org/10.1016/j.jneumeth.2008.03.013> (2008).
67. Kuroda, K. *et al.* Non-aqueous, zwitterionic solvent as an alternative for dimethyl sulfoxide in the life sciences. *Commun. Chem.* **3**, 163. <https://doi.org/10.1038/s42004-020-00409-7> (2020).
68. Waybright, T. J., Britt, J. R. & McCloud, T. G. Overcoming problems of compound storage in DMSO: Solvent and process alternatives. *J. Biomol. Screen.* **14**, 708–715. <https://doi.org/10.1177/1087057109335670> (2009).
69. Pal, R., Mamidi, M. K., Das, A. K. & Bhone, R. Diverse effects of dimethyl sulfoxide (DMSO) on the differentiation potential of human embryonic stem cells. *Arch. Toxicol.* **86**, 651–661. <https://doi.org/10.1007/s00204-011-0782-2> (2012).
70. Ohmori, L., Slepak, T. L., Bixby, J. L. & Lemmon, V. P. *Investigation of the Mechanism of Action of a Novel Kinase Inhibitor, SB-926* (Miller School of Medicine, University of Miami, 2016).
71. Mah, K. M. *et al.* Compounds co-targeting kinases in axon regulatory pathways promote regeneration and behavioral recovery after spinal cord injury in mice. *Exp. Neurol.* **355**, 114117. <https://doi.org/10.1016/j.expneurol.2022.114117> (2022).
72. Menzin, A. W., King, S. A., Aikins, J. K., Mikuta, J. J. & Rubin, S. C. Taxol (paclitaxel) was approved by FDA for the treatment of patients with recurrent ovarian cancer. *Gynecol. Oncol.* **54**, 103 (1994).
73. Shemesh, O. A. & Spira, M. E. Paclitaxel induces axonal microtubules polar reconfiguration and impaired organelle transport: Implications for the pathogenesis of paclitaxel-induced polyneuropathy. *Acta Neuropathol.* **119**, 235–248. <https://doi.org/10.1007/s00401-009-0586-0> (2010).
74. Brandolini, L. *et al.* CXCR1/2 pathways in paclitaxel-induced neuropathic pain. *Oncotarget* **8**, 23188–23201. <https://doi.org/10.18632/oncotarget.15533> (2017).
75. Cross, D. J. *et al.* Paclitaxel reduces brain injury from repeated head trauma in mice. *J. Alzheimers Dis.* **67**, 859–874. <https://doi.org/10.3233/JAD-180871> (2019).
76. Blackmore, M. G. *et al.* High content screening of cortical neurons identifies novel regulators of axon growth. *Mol. Cell Neurosci.* **44**, 43–54. <https://doi.org/10.1016/j.mcn.2010.02.002> (2010).
77. Fink, K. L., López-Giráldez, F., Kim, I. J., Strittmatter, S. M. & Cafferty, W. B. J. Identification of intrinsic axon growth modulators for intact CNS neurons after injury. *Cell Rep.* **18**, 2687–2701. <https://doi.org/10.1016/j.celrep.2017.02.058> (2017).
78. Azpurua, J. & Eaton, B. A. Neuronal epigenetics and the aging synapse. *Front. Cell. Neurosci.* **9**, 208–208. <https://doi.org/10.3389/fncel.2015.00208> (2015).
79. Li, P. *et al.* Epigenetic dysregulation of enhancers in neurons is associated with Alzheimer's disease pathology and cognitive symptoms. *Nat. Commun.* **10**, 2246. <https://doi.org/10.1038/s41467-019-10101-7> (2019).
80. Stewart, A. N. *et al.* Mitochondria exert age-divergent effects on recovery from spinal cord injury. *Exp. Neurol.* **337**, 113597–113597. <https://doi.org/10.1016/j.expneurol.2021.113597> (2021).
81. Ohsawa, F., Widmer, H. R., Knusel, B., Denton, T. L. & Hefti, F. Response of embryonic rat hippocampal neurons in culture to neurotrophin-3, brain-derived neurotrophic factor and basic fibroblast growth factor. *Neuroscience* **57**, 67–77. [https://doi.org/10.1016/0306-4522\(93\)90112-S](https://doi.org/10.1016/0306-4522(93)90112-S) (1993).
82. Wu, K. *et al.* Functional trkB neurotrophin receptors are intrinsic components of the adult brain postsynaptic density. *Brain Res. Mol. Brain Res.* **43**, 286–290. [https://doi.org/10.1016/S0169-328X\(96\)00211-2](https://doi.org/10.1016/S0169-328X(96)00211-2) (1996).

83. Neumann, H., Kotter, M. R. & Franklin, R. J. M. Debris clearance by microglia: An essential link between degeneration and regeneration. *Brain* **132**, 288–295. <https://doi.org/10.1093/brain/awn109> (2009).
84. He, B. R., Xie, S. T., Wu, M. M., Hao, D. J. & Yang, H. Phagocytic removal of neuronal debris by olfactory ensheathing cells enhances neuronal survival and neurite outgrowth via p38MAPK activity. *Mol. Neurobiol.* **49**, 1501–1512. <https://doi.org/10.1007/s12035-013-8588-2> (2014).
85. Viesselmann, C., Ballweg, J., Lombard, D. & Dent, E. W. Nucleofection and primary culture of embryonic mouse hippocampal and cortical neurons. *JoVE*. <https://doi.org/10.3791/2373> (2011).
86. Lu, Z., Piechowicz, M. & Qiu, S. A simplified method for ultra-low density, long-term primary hippocampal neuron culture. *JoVE*. <https://doi.org/10.3791/53797> (2016).
87. Cullen, D. K., Gilroy, M. E., Irons, H. R. & Laplaca, M. C. Synapse-to-neuron ratio is inversely related to neuronal density in mature neuronal cultures. *Brain Res.* **1359**, 44–55. <https://doi.org/10.1016/j.brainres.2010.08.058> (2010).
88. Biffi, E., Regalia, G., Menegon, A., Ferrigno, G. & Pedrocchi, A. The influence of neuronal density and maturation on network activity of hippocampal cell cultures: A methodological study. *PLoS ONE* **8**, e83899. <https://doi.org/10.1371/journal.pone.0083899> (2013).
89. Watanabe, M. *et al.* Glutamine is involved in the dependency of brain neuron survival on cell plating density in culture. *NeuroReport* **9**, 2353–2357. <https://doi.org/10.1097/00001756-199807130-00037> (1998).
90. Hong, Y., Zhao, T., Li, X. J. & Li, S. Mutant huntingtin impairs BDNF release from astrocytes by disrupting conversion of Rab3a-GTP into Rab3a-GDP. *J. Neurosci.* **36**, 8790–8801. <https://doi.org/10.1523/jneurosci.0168-16.2016> (2016).
91. Grasman, J. M. & Kaplan, D. L. Human endothelial cells secrete neurotrophic factors to direct axonal growth of peripheral nerves. *Sci. Rep.* **7**, 4092. <https://doi.org/10.1038/s41598-017-04460-8> (2017).
92. Granholm, A. C. *et al.* Glial cell line-derived neurotrophic factor is essential for postnatal survival of midbrain dopamine neurons. *J. Neurosci.* **20**, 3182–3190. <https://doi.org/10.1523/jneurosci.20-09-03182.2000> (2000).
93. Paulsson, M. The role of laminin in attachment, growth, and differentiation of cultured cells: A brief review. *Cytotechnology* **9**, 99–106. <https://doi.org/10.1007/BF02521736> (1992).
94. Miner, J. H. (ed.) *Current Topics in Membranes* Vol. 76, 197–229 (Academic Press, 2015).
95. Hyysalo, A. *et al.* Laminin $\alpha 5$ substrates promote survival, network formation and functional development of human pluripotent stem cell-derived neurons in vitro. *Stem Cell Res.* **24**, 118–127. <https://doi.org/10.1016/j.scr.2017.09.002> (2017).
96. Flanagan, L. A., Rebaza, L. M., Derzic, S., Schwartz, P. H. & Monuki, E. S. Regulation of human neural precursor cells by laminin and integrins. *J. Neurosci. Res.* **83**, 845–856. <https://doi.org/10.1002/jnr.20778> (2006).
97. Fawcett, J. W. An integrin approach to axon regeneration. *Eye* **31**, 206–208. <https://doi.org/10.1038/eye.2016.293> (2017).
98. Condic, M. L. Adult neuronal regeneration induced by transgenic integrin expression. *J. Neurosci.* **21**, 4782–4788. <https://doi.org/10.1523/JNEUROSCI.21-13-04782.2001> (2001).
99. Malin, S. A., Davis, B. M. & Molliver, D. C. Production of dissociated sensory neuron cultures and considerations for their use in studying neuronal function and plasticity. *Nat. Protoc.* **2**, 152–160. <https://doi.org/10.1038/nprot.2006.461> (2007).
100. Motomura, T., Hayashida, Y. & Murayama, N. Mechanical dissociation of retinal neurons with vibration. *Electron. Commun. Jpn.* **92**, 43–52. <https://doi.org/10.1002/ecj.10062> (2009).
101. Jager, L. D. *et al.* Effect of enzymatic and mechanical methods of dissociation on neural progenitor cells derived from induced pluripotent stem cells. *Adv. Med. Sci.* **61**, 78–84. <https://doi.org/10.1016/j.advms.2015.09.005> (2016).
102. Kaiser, O. *et al.* Dissociated neurons and glial cells derived from rat inferior colliculi after digestion with papain. *PLoS ONE* **8**, e80490. <https://doi.org/10.1371/journal.pone.0080490> (2013).
103. Hilgenberg, L. G. W. & Smith, M. A. Preparation of dissociated mouse cortical neuron cultures. *J. Vis. Exp.* <https://doi.org/10.3791/562> (2007).
104. Tamagnini, E., Scullion, S., Brown, J. T. & Randall, A. D. Low concentrations of the solvent dimethyl sulphoxide alter intrinsic excitability properties of cortical and hippocampal pyramidal cells. *PLoS ONE* **9**, e92557. <https://doi.org/10.1371/journal.pone.0092557> (2014).
105. Zhang, C. *et al.* Effects of dimethyl sulfoxide on the morphology and viability of primary cultured neurons and astrocytes. *Brain Res. Bull.* **128**, 34–39. <https://doi.org/10.1016/j.brainresbull.2016.11.004> (2017).
106. Wang, X. *et al.* Essential role of ERK activation in neurite outgrowth induced by α -lipoic acid. *Biochim. Biophys. Acta* **1813**, 827. <https://doi.org/10.1016/j.bbamcr.2011.01.027> (2011).
107. Elisia, I. *et al.* DMSO represses inflammatory cytokine production from human blood cells and reduces autoimmune arthritis. *PLoS ONE* **11**, e0152538. <https://doi.org/10.1371/journal.pone.0152538> (2016).
108. Giacomini, K. M. *et al.* Genome-wide association studies of drug response and toxicity: An opportunity for genome medicine. *Nat. Rev. Drug Discov.* **16**, 70–70. <https://doi.org/10.1038/nrd.2016.234> (2017).
109. Goetz, L. H. & Schork, N. J. Personalized medicine: Motivation, challenges, and progress. *Fertil. Steril.* **109**, 952–963. <https://doi.org/10.1016/j.fertnstert.2018.05.006> (2018).
110. Al-Ali, H. *et al.* The mTOR substrate S6 kinase 1 (S6K1) is a negative regulator of axon regeneration and a potential drug target for central nervous system injury. *J. Neurosci.* **37**, 7079–7095. <https://doi.org/10.1523/JNEUROSCI.0931-17.2017> (2017).
111. Lin, B., Xiong, G. & Yang, W. Ribosomal protein S6 kinase 1 promotes the survival of photoreceptors in retinitis pigmentosa. *Cell Death Dis.* **9**, 1141. <https://doi.org/10.1038/s41419-018-1198-1> (2018).
112. Park, J. *et al.* Involvement of S6K1 in mitochondria function and structure in HeLa cells. *Cell Signal* **28**, 1904–1915. <https://doi.org/10.1016/j.celsig.2016.09.003> (2016).
113. Noh, E.-M. *et al.* Skin aging-dependent activation of the PI3K signaling pathway via downregulation of PTEN increases intracellular ROS in human dermal fibroblasts. *Oxid. Med. Cell. Longev.* **2016**, 6354261. <https://doi.org/10.1155/2016/6354261> (2016).
114. Higuchi, M., Onishi, K., Masuyama, N. & Gotoh, Y. The phosphatidylinositol-3 kinase (PI3K)-Akt pathway suppresses neurite branch formation in NGF-treated PC12 cells. *Genes Cells* **8**, 657–669. <https://doi.org/10.1046/j.1365-2443.2003.00663.x> (2003).
115. Triplett, J. C. *et al.* Age-related changes in the proteostasis network in the brain of the naked mole-rat: Implications promoting healthy longevity. *Biochem. Biophys. Acta.* **1852**, 2213. <https://doi.org/10.1016/j.bbadis.2015.08.002> (2015).
116. Copp, J., Manning, G. & Hunter, T. TORC-specific phosphorylation of mammalian target of rapamycin (mTOR): Phospho-Ser2481 is a marker for intact mTOR signaling complex 2. *Can. Res.* **69**, 1821–1827. <https://doi.org/10.1158/0008-5472.CAN-08-3014> (2009).
117. Jin, Y. *et al.* Atorvastatin enhances neurite outgrowth in cortical neurons in vitro via up-regulating the Akt/mTOR and Akt/GSK-3 β signaling pathways. *Acta Pharmacol. Sin.* **33**, 861–872. <https://doi.org/10.1038/aps.2012.59> (2012).
118. Liu, S. *et al.* PTEN modulates neurites outgrowth and neuron apoptosis involving the PI3K/Akt/mTOR signaling pathway. *Mol. Med. Rep.* **20**, 4059–4066. <https://doi.org/10.3892/mmr.2019.10670> (2019).
119. Lejri, I., Grimm, A. & Eckert, A. Ginkgo biloba extract increases neurite outgrowth and activates the Akt/mTOR pathway. *PLoS ONE* **14**, e0225761. <https://doi.org/10.1371/journal.pone.0225761> (2019).
120. Hedges, C. P. *et al.* Prolonged treatment with a PI3K p110 α inhibitor causes sex- and tissue-dependent changes in antioxidant content, but does not affect mitochondrial function. *Biosci. Rep.* **40**, 20201128. <https://doi.org/10.1042/BSR20201128> (2020).
121. Cueno, M. E., Kamio, N., Seki, K., Kurita-Ochiai, T. & Ochiai, K. High butyric acid amounts induce oxidative stress, alter calcium homeostasis, and cause neurite retraction in nerve growth factor-treated PC12 cells. *Cell Stress Chaperones* **20**, 709–713. <https://doi.org/10.1007/s12192-015-0584-1> (2015).

122. Baar, E. L., Carbajal, K. A., Ong, I. M. & Lamming, D. W. Sex- and tissue-specific changes in mTOR signaling with age in C57BL/6J mice. *Aging Cell* **15**, 155–166. <https://doi.org/10.1111/accel.12425> (2016).
123. Rodriguez, K. A. *et al.* Divergent tissue and sex effects of rapamycin on the proteasome-chaperone network of old mice. *Front. Mol. Neurosci.* <https://doi.org/10.3389/fnmol.2014.00083> (2014).
124. Song, E. J., Hong, H. M. & Yoo, Y. S. Proteasome inhibition induces neurite outgrowth through posttranslational modification of TrkA receptor. *Int. J. Biochem. Cell Biol.* **41**, 539–545. <https://doi.org/10.1016/j.bio.2008.04.022> (2009).
125. Lichtman, S. M. *et al.* Paclitaxel efficacy and toxicity in older women with metastatic breast cancer: Combined analysis of CALGB 9342 and 9840. *Ann. Oncol.* **23**, 632–638. <https://doi.org/10.1093/annonc/mdr297> (2012).
126. Geula, C. *et al.* Aging renders the brain vulnerable to amyloid beta-protein neurotoxicity. *Nat. Med.* **4**, 827–831. <https://doi.org/10.1038/nm0798-827> (1998).
127. Bogers, C. H., Boshuisen, M. L., Kok, J. S. & Knegtering, H. Neurotoxicity in elderly patients being treated with lithium: Is there a reason to adjust the dosage administered? *Tijdschr. Psychiatr.* **54**, 359–369 (2012).
128. Mangoni, A. A. & Jackson, S. H. D. Age-related changes in pharmacokinetics and pharmacodynamics: Basic principles and practical applications. *Br. J. Clin. Pharmacol.* **57**, 6–14. <https://doi.org/10.1046/j.1365-2125.2003.02007.x> (2004).
129. Danik, M., Puma, C., Quirion, R. & Williams, S. Widely expressed transcripts for chemokine receptor CXCR1 in identified glutamatergic, γ -aminobutyric acidergic, and cholinergic neurons and astrocytes of the rat brain: A single-cell reverse transcription-multiplex polymerase chain reaction study. *J. Neurosci. Res.* **74**, 286–295. <https://doi.org/10.1002/jnr.10744> (2003).
130. Wheeler, H. E., Wing, C., Delaney, S. M., Komatsu, M. & Dolan, M. E. Modeling chemotherapeutic neurotoxicity with human induced pluripotent stem cell-derived neuronal cells. *PLoS ONE* **10**, e0118020. <https://doi.org/10.1371/journal.pone.0118020> (2015).
131. Hsu, Y.-C. *et al.* Signaling adaptor protein SH2B1 enhances neurite outgrowth and accelerates the maturation of human induced neurons. *Stem Cells Transl. Med.* **3**, 713–722. <https://doi.org/10.5966/sctm.2013-0111> (2014).
132. Grunwald, L.-M. *et al.* Comparative characterization of human induced pluripotent stem cells (hiPSC) derived from patients with schizophrenia and autism. *Transl. Psychiatry* **9**, 179. <https://doi.org/10.1038/s41398-019-0517-3> (2019).

Acknowledgements

This research was funded by Texas A&M start-up funds to C.G.G. We thank Vance Lemmon, John Bixby, and Hassan Al-Ali for providing the RO48 compound and for their feedback on the methodology, analysis, and the overall manuscript. We thank Dwight Baker for providing consultation on assay development, and Jim Sacchetti for the use of the TAMU High Throughput Screening (HTS) Drug Screening Lab. We thank Graphit Science & Art for preparing the illustrations used in Fig. 8.

Author contributions

A.S. and C.G.G. conceptualized, developed the methodology, designed the experiments, and wrote the manuscript. A.S. conducted all experiments. C.G.G. provided funding. I.R. provided equipment and resources to perform experiments. All authors have read and agreed to the published version of the manuscript.

Competing interests

The authors declare that the research was conducted in the absence of any commercial or financial relationships that could be construed as a potential conflict of interest. A.S. and C.G.G. currently hold pending patent applications regarding the technology listed herein and are substantial owners of NeuroCreis.

Additional information

Supplementary Information The online version contains supplementary material available at <https://doi.org/10.1038/s41598-022-17389-4>.

Correspondence and requests for materials should be addressed to C.G.G.

Reprints and permissions information is available at www.nature.com/reprints.

Publisher's note Springer Nature remains neutral with regard to jurisdictional claims in published maps and institutional affiliations.



Open Access This article is licensed under a Creative Commons Attribution 4.0 International License, which permits use, sharing, adaptation, distribution and reproduction in any medium or format, as long as you give appropriate credit to the original author(s) and the source, provide a link to the Creative Commons licence, and indicate if changes were made. The images or other third party material in this article are included in the article's Creative Commons licence, unless indicated otherwise in a credit line to the material. If material is not included in the article's Creative Commons licence and your intended use is not permitted by statutory regulation or exceeds the permitted use, you will need to obtain permission directly from the copyright holder. To view a copy of this licence, visit <http://creativecommons.org/licenses/by/4.0/>.

© The Author(s) 2022